

# Functional antibody and T-cell immunity following SARS-CoV-2 infection, including by variants of concern, in patients with cancer: the CAPTURE study

Annika Fendler  
Lewis Au  
Scott Shepherd  
Fiona Byrne  
Maddalena Cerrone  
Laura Boos  
Karolina Rzeniewicz  
William Gordon  
Ben Shum  
Camille Gerard  
Barry Ward  
Wenyi Xie  
Andreas Schmitt  
Nalinie Joharatnam-Hogan  
Georgina Cornish  
Martin Pule  
Leila Mekkaoui  
Kevin Ng  
Eleanor Carlyle  
Kim Edmonds  
Lyra Del Rosario  
Sarah Sarker  
Karla Lingard  
Mary Mangwende  
Lucy Holt  
Hamid Ahmod  
Richard Stone  
Camila Gomes  
Helen Flynn  
Ana Agua-Doce  
Philip Hobson  
Simon Caidan

Michael Howell  
Mary Wu  
Robert Goldstone  
Margaret Crawford  
Laura Cubitt  
Harshil Patel  
Mike Gavrielides  
Emma Nye  
Ambrosius Snijders  
James MacRae  
Jerome Nicod  
Firza Gronthoud  
Robyn Shea  
Christina Messiou  
David Cunningham  
Ian Chau  
Naureen Starling  
Nicholas Turner  
Liam Welsh  
Nicholas van As  
Robin Jones  
Joanne Droney  
Susana Banerjee  
Kate Tatham  
Shaman Jhanji  
Mary O'Brien  
Oliva Curtis  
Kevin Harrington  
Shreerang Bhide  
Jessica Bazin  
Anna Robinson  
Clemency Stephenson  
Tim Slattery  
Yasir Khan  
Zayd Tippu  
Isla Leslie  
Spyridon Gennatas  
Alicia Okines  
Alison Reid  
Kate Young  
Andrew Furness  
Lisa Pickering

Sonia Gandhi  
Steve Gamblin  
Charles Swanton  
Emma Nicholson  
Sacheen Kumar  
Nadia Yousaf  
Katalin Wilkinson  
Anthony Swerdlow  
Ruth Harvey  
George Kassiotis  
James Larkin  
Robert Wilkinson  
Samra Turajlic (✉ [samra.turajlic@crick.ac.uk](mailto:samra.turajlic@crick.ac.uk))

---

## Research Article

**Keywords:** SARS-CoV-2, COVID-19, Cancer, Adaptive Immunity, Antibody Response, Neutralising Antibodies, T-cell Response, Prospective Study, Vaccine

**Posted Date:** September 20th, 2021

**DOI:** <https://doi.org/10.21203/rs.3.rs-916427/v1>

**License:**  This work is licensed under a Creative Commons Attribution 4.0 International License.

[Read Full License](#)

---

**Version of Record:** A version of this preprint was published at Nature Cancer on October 27th, 2021. See the published version at <https://doi.org/10.1038/s43018-021-00275-9>.

1 **Functional antibody and T-cell immunity following SARS-CoV-2 infection,**  
2 **including by variants of concern, in patients with cancer: the CAPTURE study**

3  
4 Annika Fendler<sup>1,43</sup>, Lewis Au<sup>1,2,43</sup>, Scott T.C. Shepherd<sup>1,2,43</sup>, Fiona Byrne<sup>1</sup>, Maddalena Cerrone<sup>3,4</sup>, Laura  
5 Amanda Boos<sup>2</sup>, Karolina Rzeniewicz<sup>1</sup>, William Gordon<sup>1</sup>, Ben Shum<sup>1,2</sup>, Camille L. Gerard<sup>1</sup>, Barry Ward<sup>1</sup>,  
6 Wenyi Xie<sup>1</sup>, Andreas M. Schmitt<sup>2</sup>, Nalinie Joharatnam-Hogan<sup>2</sup>, Georgina H. Cornish<sup>5</sup>, Martin Pule<sup>6,7</sup>,  
7 Leila Mekkaoui<sup>7</sup>, Kevin W. Ng<sup>5</sup>, Eleanor Carlyle<sup>2</sup>, Kim Edmonds<sup>2</sup>, Lyra Del Rosario<sup>2</sup>, Sarah Sarker<sup>2</sup>,  
8 Karla Lingard<sup>2</sup>, Mary Mangwende<sup>2</sup>, Lucy Holt<sup>2</sup>, Hamid Ahmod<sup>2</sup>, Richard Stone<sup>7</sup>, Camila Gomes<sup>7</sup>, Helen  
9 R. Flynn<sup>9</sup>, Ana Agua-Doce<sup>10</sup>, Philip Hobson<sup>10</sup>, Simon Caidan<sup>11</sup>, Michael Howell<sup>12</sup>, Mary Wu<sup>12</sup>, Robert  
10 Goldstone<sup>13</sup>, Margaret Crawford<sup>13</sup>, Laura Cubitt<sup>13</sup>, Harshil Patel<sup>14</sup>, Mike Gavrielides<sup>15</sup>, Emma Nye<sup>8</sup>,  
11 Ambrosius P Snijders<sup>9</sup>, James I MacRae<sup>16</sup>, Jerome Nicod<sup>13</sup>, Firza Gronthoud<sup>17</sup>, Robyn L. Shea<sup>17,18</sup>,  
12 Christina Messiou<sup>19</sup>, David Cunningham<sup>20</sup>, Ian Chau<sup>20</sup>, Naureen Starling<sup>20</sup>, Nicholas Turner<sup>21</sup>, Liam  
13 Welsh<sup>22</sup>, Nicholas van As<sup>23</sup>, Robin L. Jones<sup>24</sup>, Joanne Droney<sup>25</sup>, Susana Banerjee<sup>26</sup>, Kate C. Tatham<sup>27</sup>,  
14 Shaman Jhanji<sup>27</sup>, Mary O'Brien<sup>28</sup>, Olivia Curtis<sup>28</sup>, Kevin Harrington<sup>29,30</sup>, Shreerang Bhide<sup>29</sup>, Jessica  
15 Bazin<sup>31</sup>, Anna Robinson<sup>31</sup>, Clemency Stephenson<sup>31</sup>, Tim Slattery<sup>2</sup>, Yasir Khan<sup>2</sup>, Zayd Tippu<sup>2</sup>, Isla  
16 Leslie<sup>2</sup>, Spyridon Gennatas<sup>32,33</sup>, Alicia Okines<sup>21,32</sup>, Alison Reid<sup>34</sup>, Kate Young<sup>2</sup>, Andrew J.S. Furness<sup>2</sup>,  
17 Lisa Pickering<sup>2</sup>, Sonia Gandhi<sup>35,36</sup>, Steve Gamblin<sup>37</sup>, Charles Swanton<sup>38,39</sup> on behalf of the Crick  
18 COVID19 consortium, Emma Nicholson<sup>31</sup>, Sacheen Kumar<sup>20</sup>, Nadia Yousaf<sup>28,32</sup>, Katalin A. Wilkinson<sup>3,42</sup>,  
19 Anthony Swerdlow<sup>40</sup>, Ruth Harvey<sup>41</sup>, George Kassiotis<sup>5</sup>, James Larkin<sup>2</sup>, Robert J. Wilkinson<sup>3,4,42</sup>, Samra  
20 Turajlic<sup>1,2,\*</sup> on behalf of the CAPTURE consortium

21  
22 <sup>1</sup>Cancer Dynamics Laboratory, The Francis Crick Institute, London, NW1 1AT, UK

23 <sup>2</sup>Skin and Renal Units, The Royal Marsden NHS Foundation Trust, London, SW3 6JJ, UK

24 <sup>3</sup>Tuberculosis Laboratory, The Francis Crick Institute, London, NW1 1AT, UK

25 <sup>4</sup>Department of Infectious Disease, Imperial College London, W12 0NN, UK

26 <sup>5</sup>Retroviral Immunology Laboratory, The Francis Crick Institute, London, NW1 1AT, UK

27 <sup>6</sup>Research Department of Haematology at University College London Cancer Institute, WC1E 6DD,  
28 London, UK

29 <sup>7</sup>Autolus Limited, The MediaWorks, 191 Wood Lane, London, W12 7F

30 <sup>8</sup>Experimental Histopathology Laboratory, The Francis Crick Institute, London, NW1 1AT, UK

31 <sup>9</sup>Mass Spectrometry Proteomics Science Technology Platform, The Francis Crick Institute, London,  
32 NW1 1AT, UK

33 <sup>10</sup>Flow Cytometry Scientific Technology Platform, The Francis Crick Institute, London, NW1 1AT, UK

34 <sup>11</sup>Safety, Health & Sustainability, The Francis Crick Institute, London, NW1 1AT, UK  
35 <sup>12</sup>High Throughput Screening Laboratory, The Francis Crick Institute, London, NW1 1AT, UK  
36 <sup>13</sup>Advanced Sequencing Facility, The Francis Crick Institute, London, NW1 1AT, UK  
37 <sup>14</sup>Department of Bioinformatics and Biostatistics, The Francis Crick Institute, London, UK.  
38 <sup>15</sup>Scientific Computing Scientific Technology Platform, The Francis Crick Institute, London, NW1 1AT,  
39 UK  
40 <sup>16</sup>Metabolomics Scientific Technology Platform, The Francis Crick Institute, London, NW1 1AT, UK  
41 <sup>17</sup>Department of Pathology, The Royal Marsden NHS Foundation Trust, London, NW1 1AT, UK  
42 <sup>18</sup>Translational Cancer Biochemistry Laboratory, The Institute of Cancer Research, London, SW7 3RP,  
43 UK  
44 <sup>19</sup>Department of Radiology, The Royal Marsden NHS Foundation Trust, London, SW3 6JJ, UK  
45 <sup>20</sup>Gastrointestinal Unit, The Royal Marsden NHS Foundation Trust, London and Surrey SM2 5PT  
46 <sup>21</sup>Breast Unit, The Royal Marsden NHS Foundation Trust, London, SW3 6JJ, UK  
47 <sup>22</sup>Neuro-oncology Unit, The Royal Marsden NHS Foundation Trust, London, SW3 6JJ, UK  
48 <sup>23</sup>Clinical Oncology Unit, The Royal Marsden NHS Foundation Trust, London, SW3 6JJ, UK  
49 <sup>24</sup>Sarcoma Unit, The Royal Marsden NHS Foundation Trust and Institute of Cancer Research, London,  
50 SW3 6JJ, UK  
51 <sup>25</sup>Palliative Medicine, The Royal Marsden NHS Foundation Trust, London, SW3 6JJ, UK  
52 <sup>26</sup>Gynaecology Unit, The Royal Marsden NHS Foundation Trust, London, SW3 6JJ, UK  
53 <sup>27</sup>Anaesthetics, Perioperative Medicine and Pain Department, The Royal Marsden NHS Foundation  
54 Trust, London, SW3 6JJ, UK  
55 <sup>28</sup>Lung Unit, The Royal Marsden NHS Foundation Trust, London, SW3 6JJ, UK  
56 <sup>29</sup>Head and Neck, The Royal Marsden NHS Foundation Trust, London, SW3 6JJ, UK  
57 <sup>30</sup>Targeted Therapy Team, The Institute of Cancer Research, London, SW7 3RP, UK  
58 <sup>31</sup>Haemato-oncology Unit, The Royal Marsden NHS Foundation Trust, London, SW3 6JJ, UK  
59 <sup>32</sup>Acute Oncology Service, The Royal Marsden NHS Foundation Trust, London, SW3 6JJ, UK  
60 <sup>33</sup>Department of Medical Oncology, 14th Floor, Great Maze Pond Road, Tower Wing, Guy's Hospital,  
61 London SE1 9RY, UK  
62 <sup>34</sup>Uro-oncology unit, The Royal Marsden NHS Foundation Trust, Surrey, SM2 5PT  
63 <sup>35</sup>Neurodegeneration Biology Laboratory, The Francis Crick Institute, London, NW1 1AT, UK  
64 <sup>36</sup>UCL Queen Square Institute of Neurology, Queen Square, London WC1N 3BG  
65 <sup>37</sup>Structural Biology of Disease Processes Laboratory, The Francis Crick Institute, London, NW1 1AT,  
66 UK

67 <sup>38</sup>Cancer Evolution and Genome Instability Laboratory, The Francis Crick Institute, London, NW1 1AT,

68 UK

69 <sup>39</sup>University College London Cancer Institute, London WC1E 6DD, UK

70 <sup>40</sup>Division of Genetics and Epidemiology and Division of Breast Cancer Research, The Institute of

71 Cancer Research, London, SW7 3RP, UK

72 <sup>41</sup>Worldwide Influenza Centre, The Francis Crick Institute, London, NW1 1AT, UK

73 <sup>42</sup>Wellcome Center for Infectious Disease Research in Africa, University Cape Town, Observatory

74 7925, Republic of South Africa

75 <sup>43</sup>Equal contribution

76

77

78

79 **Keywords:** SARS-CoV-2, COVID-19, Cancer, Adaptive Immunity, Antibody Response, Neutralising

80 Antibodies, T-cell Response, Prospective Study, Vaccine

81

82

83 **\*Corresponding author:** Dr Samra Turajlic

84 Telephone: +44 020 37961111

85 E-mail: [samra.turajlic@crick.ac.uk](mailto:samra.turajlic@crick.ac.uk)

86

87

88

89

90 **Abstract**

91 Patients with cancer have higher COVID-19 morbidity and mortality. Here we present the  
92 prospective CAPTURE study (NCT03226886) integrating longitudinal immune profiling with clinical  
93 annotation. Of 357 patients with cancer, 118 were SARS-CoV-2-positive, 94 were symptomatic and 2  
94 patients died of COVID-19. In this cohort, 83% patients had S1-reactive antibodies, 82% had  
95 neutralizing antibodies against WT, whereas neutralizing antibody titers (NAbT) against the Alpha,  
96 Beta, and Delta variants were substantially reduced. Whereas S1-reactive antibody levels decreased  
97 in 13% of patients, NAbT remained stable up to 329 days. Patients also had detectable SARS-CoV-2-  
98 specific T cells and CD4+ responses correlating with S1-reactive antibody levels, although patients  
99 with hematological malignancies had impaired immune responses that were disease and treatment-  
100 specific, but presented compensatory cellular responses, further supported by clinical. Overall, these  
101 findings advance the understanding of the nature and duration of immune response to SARS-CoV-2  
102 in patients with cancer.

103  
104  
105  
106  
107  
108  
109  
110  
111  
112  
113  
114  
115  
116  
117  
118  
119  
120  
121

122 **Introduction**

123 Patients with cancer have an increased risk of severe outcomes from coronavirus disease 2019  
124 (COVID-19),<sup>1,2</sup> with risk factors including general (e.g. increased age, male sex, obesity, co-  
125 morbidities) as well as cancer-specific features (e.g. haematological and thoracic malignancies,  
126 active cancer, poor performance status).<sup>3-8</sup> The precise effects of anti-cancer treatments on the  
127 course and outcome of SARS-CoV-2 infection are yet to be fully understood, with different reports  
128 yielding conflicting results.<sup>5,7,9,10</sup> Understanding of the immune response to SARS-CoV-2 in this  
129 heterogeneous population, spanning multiple malignancy types and numerous treatment regimens,  
130 is crucial for optimal clinical management of those patients during the ongoing pandemic.

131 Calibration of current and future risk-mitigation measures, including risk of re-infection and  
132 vaccine effectiveness, requires an understanding of the impact of cancer and cancer treatments on  
133 the nature, extent and duration of immunity to SARS-CoV-2. Previous studies established an acute  
134 immune response to SARS-CoV-2 in cancer patients, with 1) solid tumour patients showing high  
135 seroconversion rates, and 2) haematological cancer patients showing impaired humoral immunity,  
136 especially under anti-CD20 treatments, but with improved survival in those with higher CD8+ T-cell  
137 counts.<sup>11-13</sup> However, features of the immune response (including SARS-CoV-2-specific T-cells and  
138 neutralising antibodies), and their correlation with clinical characteristics in large non-hospitalized  
139 cancer cohorts, and cross-protection against emerging variants of concern (VOC) remain unknown.

140 CAPTURE (COVID-19 antiviral response in a pan-tumour immune monitoring study) is a  
141 prospective, longitudinal cohort study initiated in response to the global SARS-CoV-2 pandemic and  
142 its impact on cancer patients.<sup>14</sup> The study evaluates the impact of cancer and cancer therapies on  
143 the immune response to SARS-CoV-2 infection and COVID-19 vaccinations. Here, we report findings  
144 from the SARS-CoV-2 infection cohort of the study.

145



## 146 **Results**

### 147 **Patient demographics and baseline characteristics**

148 Between May 4, 2020 and March 31st 2021 (database lock), 357 unvaccinated cancer patients were  
149 evaluable and followed-up for a median of 154 days (IQR: 63-273). Median age was 59 years, 54%  
150 were male, 89% had solid malignancy, and the majority (64%) had advanced disease (**Table 1**).  
151 Overall, 118 patients (33%; 97 with solid cancers and 21 with haematological malignancies), were  
152 classified as SARS-CoV-2-positive according to our case definition (positive SARS-CoV-2 RT-PCR  
153 and/or ELISA for S1-reactive antibodies, at/or prior to study enrolment), and were included in the  
154 analysis (**Figure 1a,b, see Methods**). The most common comorbidities were hypertension (27%),  
155 obesity (21%) and diabetes mellitus (11%); no significant baseline differences were observed  
156 between patients with solid and haematological malignancies (**Table 2, Supplementary Table 1**).  
157 Overall, 88% patients received SACT (51% chemotherapy; 21% targeted therapy; 12% immune  
158 checkpoint inhibitors [CPI]; 5% anti-CD20), 10% had radiotherapy and 13% underwent surgery in the  
159 12 weeks prior to infection. Response to the most recent anti-cancer intervention is shown in **Table**  
160 **2**.

161

### 162 **Viral shedding and lineage**

163 SARS-CoV-2 infection was confirmed by SARS-CoV-2 RT-PCR in 95/118 patients (81%). Repeat testing  
164 was not mandated by study protocol but 40% (47/118) had longitudinal swabs in the course of  
165 routine care. Within this group, the estimated median duration of viral shedding (see **Methods**) was  
166 12 days (range: 6-80) (**Figure 1c, Table 3**), with evidence of prolonged shedding in patients with  
167 haematological malignancies (median 21 vs 12 days in patients with solid cancers) (**Extended Data**  
168 **Figure 1a**). Duration of viral shedding was not correlated with COVID-19 severity ( $r = 0.04$ ,  $p = 0.7$ ).  
169 We performed viral sequencing in 52 RT-PCR-positive samples with Ct > 32, of which 44/52 passed  
170 sequencing quality control. The Alpha VOC accounted for the majority of infections in our cohort  
171 between December 2020 and March 2021, consistent with community prevalence in the UK  
172 (**Extended Data Figure 1b**).

173

### 174 **Clinical correlates of COVID-19 severity in cancer patients**

175 Overall, 94 patients (80%) were symptomatic, of whom 52 (44%) had mild, 36 (31%) moderate, and 6  
176 (5%) severe illness (as per the WHO severity scale,<sup>15</sup> **Table 3**); 24 patients (20%) were asymptomatic  
177 (WHO score 1). Among all patients (n=118), fever (47%), cough (42%), gastro-intestinal symptoms  
178 (12%), and dyspnoea (31%) were the most common presenting symptoms (**Figure 1d**), with a  
179 median of 2 symptoms reported (range: 0-7). In patients with a clear date of symptom resolution

180 (n=77), duration of symptoms was 18 days (IQR: 11-30). Three patients met the criteria of long  
181 COVID (symptomatic > 90 days since presentation of disease (POD)), all following severe COVID-19  
182 requiring ITU care.

183 Thirty-three patients (28%) were hospitalised due to COVID-19, with a median duration of  
184 in-patient stay of nine days (range: 1-120); 27 (23%) required supplemental oxygen, seven (6%) were  
185 admitted to an intensive care unit (ICU), with one (1%) requiring mechanical ventilation and  
186 inotropic support (**Table 3**). Thirteen patients (11%) were treated with corticosteroids (>10 mg  
187 prednisolone equivalent), and three patients (3%) received tocilizumab. Nine patients (8%) had a  
188 thrombo-embolic complication. At database lock, eleven SARS-CoV-2-positive patients (9%) died of  
189 progressive cancer, and two patients (2%) died due to recognised complications of COVID-19 (**Table**  
190 **3**).

191 The risk of moderate and severe COVID-19 was associated with haematological  
192 malignancies, while risk of severe COVID-19 in solid malignancies was associated with progressive  
193 disease under SACT (**Supplementary Table 2**), in line with previous reports<sup>7,8,12</sup>. We found no  
194 association between COVID-19 severity, cancer stage, performance status, sex, age, obesity, smoking  
195 status or comorbidities across the whole cohort, though positive association of these factors were  
196 noted in registries largely reporting on cancer patients hospitalised with COVID-19<sup>4,7,8,16,17</sup>.

197

### 198 **Cytokine profiles and disease severity during infection**

199 Due to the study design, recruitment was biased towards patients within the convalescent stage of  
200 infection. Twenty-seven patients (23%) were recruited while being RT-PCR-positive, and three (3%)  
201 became RT-PCR-positive after recruitment to CAPTURE. Cyto/chemokine profiling of 13 patients with  
202 acute infection (8 solid tumour, 6 haematological malignancy) indicated that IL-6, IL-8 IFN- $\gamma$ , IL-18, IL-  
203 9, IP-10, and MIP1-Beta levels were elevated compared to control (**Extended Data Figure 1c,d, see**  
204 **Methods**) and correlated with severe disease (**Extended Data Figure 1e,f**). Concentration of IFN- $\gamma$   
205 and IL-18 in serum was significantly higher in patients with haematological malignancies<sup>18</sup> (**Extended**  
206 **Data Figure 1g**).

207

### 208 **S1-reactive SARS-CoV-2 antibody response in cancer patients**

209 We evaluated total S1-reactive antibody titres by ELISA at multiple time-points throughout the study  
210 (with two median samples per patient [range: 1-10]). In total, 97/118 patients (82%) tested positive  
211 (85/95 [89%] solid tumours, 12/21 [57%] haematological malignancy); blood samples were not  
212 available for 2/118 patients (2%). Overall, 76/94 (81%) symptomatic and 21/24 (88%) asymptomatic  
213 patients had S1-reactive antibodies, and among the symptomatic patients there was a non-

214 significant trend for higher S1-reactive antibody titres in those with higher COVID-19 severity ( $P =$   
215 0.057) (**Figure 2a**).

216 Thirteen patients (11%), with median follow up of 49 days (range: 14-344), had no evidence  
217 of S1-reactive antibodies but were positive by SARS-CoV-2 RT-PCR. Six further patients without  
218 detectable S1 antibody had no follow-up. Lack of seroconversion was significantly associated with  
219 haematological malignancies: 9/21 patients (43%) with haematological vs 10/97 patients (10%) with  
220 solid malignancies did not seroconvert ( $p = 0.0012$ ). Antibody titres were also significantly lower in  
221 patients with haematological malignancies (**Figure 2b**). Two patients with long COVID did not  
222 seroconvert at any point during follow up.

223 A sensitive flow cytometric assay conducted on sera from a subset of patients with S1-  
224 reactive antibodies ( $n=40$ ; **Extended Data Figures 2a and 3**), detected S-specific IgG in 38/40 (95%)  
225 (**Extended Data Figure 2b**) and IgM in 23/40 patients (58%) (**Extended Data Figure 2c**), with levels  
226 significantly correlated with S1-reactive antibody titres ( $P < 0.0001$ ) (**Extended Data Figure 2e-f**). S-  
227 reactive IgA was detected in serum of only four patients (10%) (**Extended Data Figure 2d**), consistent  
228 with the role of IgA in early response to SARS-CoV-2 infection.<sup>18</sup>

229 Finally, we evaluated matched pre-pandemic sera from 47 patients, 10 with and 37 without  
230 S1-reactive antibodies in their sample collected during the pandemic. We found no evidence of S1-  
231 reactive antibodies in the pre-pandemic sera in any patient (**Extended Data Figure 2g**), but S-  
232 reactive IgG or IgM were detected in 18 patients without S1-reactive antibodies indicating cross-  
233 reactivity to seasonal human coronaviruses.

234

### 235 **NABs against SARS-CoV-2 VOCs in cancer patients**

236 We next performed a live virus neutralisation assay to evaluate whether patients' sera could  
237 neutralise SARS-CoV-2 (see **Methods**). We measured either neutralising activity against wild-type  
238 (WT) SARS-CoV-2 or Alpha VOC, according to the causative variant (see **Methods**). We detected  
239 neutralising antibody (NAb) activity in 84/97 patients (87%) with S1-reactive antibodies (75/85 [88%]  
240 solid tumours, 8/12 [67%] haematological malignancy), with no significant differences in NAb titres  
241 (NAbT) by COVID-19 severity (**Figure 2c**). NAbT against WT were significantly lower in patients with  
242 haematological malignancies (**Figure 2d**). In a binary logistic regression model including all cancer  
243 patients ( $n=118$ ), presence of haematological malignancy, but not comorbidities, age, sex, or COVID-  
244 19 severity was associated with lack of NAb (**Figure 2e**). In patients with solid tumours ( $n=97$ ), there  
245 was no association with cancer type, stage, progressive disease or cancer therapy (**Figure 2f,g**). We  
246 were underpowered to evaluate patients with haematological malignancies ( $n=21$ ), within a  
247 multivariate model.

248 In a subset of NAb-positive patients (N=34, 31 with solid malignancies, 3 with  
249 haematological malignancies; 25 with WT SARS-CoV-2 and 9 with Alpha VOC infection), we  
250 compared NAb against WT, Alpha, Beta, and Delta. In patients with WT infection, overall lower  
251 proportions of detectable responses (100% WT, 96% Alpha, 88% Beta, 85% Delta) were seen for VOC  
252 as well as lower NAbT vs the WT strain (**Figure 2h**). Considering patients with Alpha VOC infection,  
253 NAbT against Alpha VOC were increased vs WT and titres against Beta and Delta decreased vs. WT  
254 and Alpha.

255 There was a significant correlation between S1-reactive and NAbT for all variants ( $P < 0.01$ )  
256 (**Extended Data Figure 2h**); but we note that presence of S1-reactive antibodies was not always  
257 predictive of neutralising response, especially to VOCs.

258

### 259 **SARS-CoV-2 antibody response lasts up to 11 months**

260 Next, we assessed antibody kinetics in 81/97 patients with S1-reactive antibodies and known  
261 timing of POD (n=70 solid tumours, n=11 haematological malignancy). We analysed a median of two  
262 timepoints per patient (range: 1-10) at a median follow-up of 56 days after POD (range: 1-344).  
263 Seventy-seven (95%) had S1-reactive antibodies at the time of enrolment (median 51 days after  
264 POD, range: 1-292, **Figure 2f**). Four patients (5%) had no antibodies at enrolment, but seroconverted  
265 between day 13-117 days POD. S1-reactive antibody titres showed a weak declining trend and 12  
266 patients (15%) became seronegative 24-321 days POD: one T-ALL patient who following COVID-19  
267 had a stem cell transplant complicated by chronic graft-versus-host disease, and 11 solid tumour  
268 patients with no unifying features to account for shorter-lived antibody response. Neutralising  
269 antibodies were detected as early as day one (**Figure 2g**), and as late as day 292 after POD and  
270 remained stable up to 329 days.

271

### 272 **SARS-CoV-2-specific T-cells are detected in cancer patients**

273 PBMC stimulation assays (see **Methods**) were performed in 104/118 SARS-CoV-positive  
274 patients (n=83 solid tumour, n=21 haematological malignancy; **Extended Data Figure 3b**); 14  
275 samples were excluded (for lack or low PBMC counts). SARS-CoV-2-specific CD4<sup>+</sup> and CD8<sup>+</sup> T-cells  
276 (SsT-cells; identified by activation induced markers OX40, CD137, and CD69)<sup>19</sup> were measured  
277 (**Figure 3a,b**) at the first time point post-seroconversion (where evident), at the median of 54 days  
278 after POD (range: 1-292). We detected CD4<sup>+</sup> T-cells in 79/104 (76%), and CD8<sup>+</sup> T-cells and 54/104  
279 patients (52%) (**Figure 3c-f**). CD4<sup>+</sup> T-cells were detected in 81% of patients with solid malignancies,  
280 and in 41% of patients with haematological malignancies (**Figure 3c,e**). CD8<sup>+</sup> T-cells were detected at  
281 similar frequencies (53% and 48%) across both malignancy types (**Figure 3d,f**) at a level consistently

282 lower than CD4+ T-cells (**Extended Data Figure 4a**). The differences between CD8<sup>+</sup> and CD4<sup>+</sup> T-cell  
283 responses may be due to using 15-mer peptide pools for stimulation, though we note similar  
284 findings in non-cancer patients,<sup>20,21,22</sup> indicating potential other factors, such as the broader range of  
285 antigens that induce CD8<sup>+</sup> T-cells compared to CD4<sup>+</sup> T-cells.<sup>19</sup>

286 Consistent with functional activation, IFN- $\gamma$  secreted by SsT-cells,<sup>23</sup> was detected after *in*  
287 *vitro* stimulation, and IFN- $\gamma$  concentrations correlated with the number of SsT-cells (**Extended Data**  
288 **Figure 4b**).

289 Finally, as cross-reactive T-cell responses to HCoVs are observed frequently in healthy  
290 individuals,<sup>19,24</sup> and given the lack of matched pre-infection samples in our cohort, we extended the  
291 T-cell assay to 12 cancer patients without confirmed SARS-CoV-2 infection. Cross-reactive CD4<sup>+</sup> T-  
292 cells were detected in 7/12 and CD8<sup>+</sup> T-cells in 3/12 participants, though the overall proportion of  
293 reactive T-cells was significantly lower than in patients with confirmed SARS-CoV-2 infection ( $P < 0.05$ )  
294 (**Extended Data Figure 4c,d**).

295

#### 296 **SsT-cell compensation in patients without humoral response**

297 Patients with haematological malignancies had a wide range of antibodies (**Figure 4a,b**) and SsT-cell  
298 responses. In patients with leukaemia, NAb were detected in 6/11 and SsT-cells in 5/10 evaluable  
299 patients (two had both CD4+ and CD8+, two had CD4+ only, and one had CD8+ only). In patients  
300 with myeloma, 2/4 had NAb, and 3/4 had detectable SsT-cells (two both CD4+ and CD8+, one CD4+  
301 only). None of the six lymphoma patients, including five who were treated with anti-CD20, had  
302 detectable NAb, while SsT-cells were detected in 5/6 (three had both CD4+ and CD8+, one had  
303 CD4+ only, and one had CD8+ only). One further patient with AML treated with anti-CD20 had  
304 neither NAb nor SsT-cell responses. In total, we observed a discordance between antibody and T-cell  
305 responses amongst patients with haematological malignancy, whereby 7/9 patients with NAb to  
306 WT SARS-CoV-2 lacked SsT-cell response (CD4+ and/or CD8+), and in 12 patients without NAb  
307 activity 7 had SsT-cell response. (**Figure 4c,d, Supplementary Table 3**). Overall, the levels of SsT-cells  
308 were higher in patients with lymphomas vs leukaemias (**Figure 4e**). The highest levels of SsT-cells  
309 was observed in a patient with diffuse large B-cell lymphoma and recent anti-CD20 therapy who had  
310 no detectable neutralising antibodies.

311 In patients with solid malignancies, the level of SsT-cells did not differ significantly by  
312 tumour type (**Figure 4f**) and the level of SARS-CoV-2-reactive CD4+ T-cells was positively correlated  
313 with S1-reactive antibody titres (**Extended Data Figure 4e**), which was not observed in patients with  
314 haematological malignancies (**Extended Data Figure 4f**). However, amongst 7/10 solid tumour  
315 patients without NAb response, 5 had detectable SsT-cells (3 both CD4+ and CD8+, 2 CD4+ only,

316 **Supplementary Table 2**). Finally, following stimulation with S- and N- pools we observe that patients  
317 with haematological malignancy exhibit higher level of N-reactive compared to S-reactive CD8+ T-  
318 cells, (**Figure 4e,f**), while similar levels are observed in solid cancer patients (**Figure 4c,d**).

319

#### 320 **T-cell responses are impacted in CPI-treated patients**

321 Next, we evaluated features associated with impaired T-cell responses to SARS-CoV-2 in  
322 cancer patients. We found no association between lack of SsT-cells with the presence of solid or  
323 haematological malignancies, nor with the number of comorbidities, age, sex, or COVID-19 severity  
324 (**Figure 5a,b**). In patients with solid malignancies, those on CPI (n=14) had significantly reduced levels  
325 of SARS-CoV-2 reactive CD4+ T-cells (**Figure 5e**), and in binary logistic regression model lack of SARS-  
326 CoV-2 reactive CD4+ (but not CD8+) T-cells was associated with CPI therapy within three months of  
327 SARS-CoV-2 infection (**Figure 5c,d**). Within the patients with haematological malignancies (n=21),  
328 anti-CD20 (n=4) was not associated with obvious reduction of SARS-CoV-2 reactive T-cells (**Figure 5f**).

## 329 Discussion

330 Results from this prospective, longitudinal study of 118 SARS-CoV-2-positive cancer patients  
331 indicated that most patients with solid tumours developed a functional and durable (at least 11  
332 months) humoral immune response to SARS-CoV-2 infection, as well as an anti-SARS-CoV-2-specific  
333 T-cell response. Patients with haematological malignancies had significantly lower seroconversion  
334 rates, and impaired immune responses that were both disease- and treatment-related (anti-CD20),  
335 although with evidence of compensation.

336 Most patients (82%) in our study had solid tumours and so findings largely reflect this cancer  
337 population. The majority (89%) of solid cancer patients seroconverted following SARS-CoV-2  
338 infection (as evidenced by the presence of S1-reactive antibodies). Delayed/lack of seroconversion  
339 was observed in 10% of solid tumour patients, but no shared characteristics were identified among  
340 them. The observed high seroconversion rates in solid tumour patients were in line with data  
341 reported from smaller prospective studies conducted in the UK (95%, n=22)<sup>12</sup> and Italy (88%,  
342 n=28);<sup>25</sup> in both those studies seroconversion rates were similar to those observed in individuals  
343 without cancer. Recent studies in non-cancer subjects found a clear relationship between  
344 neutralising responses and vaccine efficacy.<sup>26,27</sup> We now showed that 88% of seroconverted solid  
345 tumour patients also had functionally relevant NAb (against WT SARS-CoV-2 or Alpha, according to  
346 the causative variant). Importantly, whilst we observed a weak decline in S1-reactive antibody titres,  
347 NAbT were stable for up to 11 months of follow-up. In non-cancer population, inconsistent results  
348 have been reported regarding the length of persistence of both SARS-CoV-2-specific IgG and NAb  
349 over time,<sup>20,28-31</sup> thus it is challenging to relate our data to those prior reports. In line with data for  
350 non-cancer SARS-CoV-2 convalescent patients<sup>32</sup>, we found that neutralising activity against Alpha,  
351 Beta, and Delta VOCs was decreased. This raises concerns about the ability of natural immunity to  
352 one variant to protect against other VOCs. Given the majority of cancer patients would now have  
353 been vaccinated against COVID-19, protection against evolving variants is critically relevant in the  
354 context of COVID-19 vaccine-induced immunity (companion paper Fender *et al.*)

355 SARS-CoV-2-infected cancer patients were previously shown to have depleted T-cells which  
356 showed markers of activation and exhaustion, and correlated with COVID-19 severity, but SsTcells  
357 were not evaluated.<sup>12</sup> In our cohort, at a median of 54 days after POD, SsT-cells (including functional  
358 IFN- $\gamma$  expressing SsT-cells) were present in the majority of evaluated solid cancer patients (76%) and  
359 in half of the haematological malignancy patients (52%). Both in the acute and convalescent phase  
360 of SARS-CoV-2 infection, a significant proportion of SARS-CoV-2-specific CD4<sup>+</sup> T-cells are T follicular  
361 helper cells (Tfh)<sup>21,33</sup> which are required for IgG and neutralising response by B-cells.<sup>34</sup> In our study,  
362 the number of CD4<sup>+</sup> T-cells was significantly correlated with S1-reactive antibody titres in solid

363 tumours, suggesting it may reflect Tfh T-cell activation and resulting B-cell activation. Overall, we  
364 found no variables associating with impaired T-cell responses to SARS-CoV-2 in cancer patients,  
365 except for CPI therapy within three months of SARS-CoV-2 infection (in solid tumours). It was  
366 previously shown that PD-1 blockade during acute viral infection can increase viral clearance by  
367 promoting CD8+ T-cell proliferation, but can also impair CD8+ T-cell memory differentiation, thereby  
368 impairing long-term immunity.<sup>35</sup> While the role of PD-1 blockade on CD4+ T-cells during acute  
369 infection is less well understood, PD-1 signalling regulates expansion of CD4+ T-cells upon an  
370 immunogenic stimulus.<sup>36</sup>

371 We found an inverse relationship between antibody and SsT-cell responses in patients with  
372 haematological malignancies, whereby leukaemia patients had more pronounced antibody but  
373 impaired SsT-cell responses, while the opposite was observed for lymphoma patients. Generally, in  
374 patients with haematological malignancies immune responses were partially compensated, i.e. more  
375 robust SsT-cell responses, especially CD8+ T-cell responses, were detected in patients without  
376 antibody responses and vice versa. Furthermore, we found SsTcells in 4/5 evaluable patients on anti-  
377 CD20 treatment, of whom none had humoral responses. In total, all but one patient with  
378 haematological malignancies had mild or moderate disease, suggesting that SsT-cell responses,  
379 specifically CD8+ T-cells and non-spike-specific SsT-cells, can at least partially compensate for lacking  
380 humoral responses, although we note our cohort was largely convalescent. In one recent study,  
381 10/13 patients with haematological malignancy and COVID-19 had SsT-cells, which were associated  
382 with improved survival (including in those on anti-CD20 therapy).<sup>11</sup> Overall, the emerging data from  
383 our study and others<sup>37</sup> appear to suggest that T-cell responses are likely important in those with  
384 haematological malignancies and may offer protection from severe COVID-19 in the absence of  
385 humoral responses.

386 The role of T-cells in protection from SARS-CoV-2 is not well understood, but T-cells were  
387 shown to play a crucial role in the clearance of acute SARS-CoV infection in mice.<sup>38</sup> In line with this,  
388 early induction of functional SsT-cells was demonstrated to associate with rapid viral clearance and  
389 mild disease in COVID-19 patients,<sup>39</sup> and preclinical animal studies suggest a role for cellular  
390 immunity in SARS-CoV-2 clearance.<sup>40</sup> Importantly, SsTcells were shown to be induced by COVID-19  
391 vaccines in both non-cancer<sup>41,42</sup> and cancer (companion paper Fender *et al.*) population, and to have  
392 activity against VOCs.<sup>43</sup> Furthermore, VOCs are not expected to escape SsTcell responses due to  
393 their highly multi-antigenic and multi-specific properties.<sup>43</sup> In the general population, data indicate  
394 that SARS-CoV-2-specific memory T-cells are maintained beyond eight months following  
395 infection.<sup>20,44</sup> In the context of the outbreak of SARS in 2003, SARS-specific T-cells were detected up  
396 to 17 years after infection, much longer than antibodies.<sup>45</sup> An ongoing aim of the CAPTURE study is



397 to evaluate the nature, durability, and clinical correlates of SsT-cell response in cancer patients as  
398 the pandemic evolves, especially in the context of COVID-19 vaccines.

399 This report has several limitations. Firstly, lack of a matched non-cancer cohort prevents  
400 direct comparisons between populations with and without cancer. Secondly, as mentioned above,  
401 the way patients are recruited into CAPTURE, including in the course of routine clinical care, may  
402 introduce selection bias, and thus our findings may not be fully generalizable to the wider cancer  
403 population. The fact that we recorded only two COVID-19-related deaths may be reflective of this (as  
404 well as the relatively low proportion of lung and haematological malignancies – the two cancer  
405 groups with increased COVID-19-related mortality).<sup>3-6</sup> Furthermore, all but one patient with  
406 haematological malignancies in our cohort recovered, while 11/18 patients with blood cancers died  
407 due to COVID-19 at our institution<sup>46</sup> before enrolment into CAPTURE commenced. Thus, it is possible  
408 that the patients with haematological malignancy in our analysis are not entirely representative of  
409 this population. Additional limitation pertains to our SsT-cell assessment - this was performed at a  
410 single time-point and so in instances where we did not detect a response, this might represent a  
411 timing bias rather than a lack of capacity to develop a response *per se*. As recruitment to CAPTURE  
412 commenced in May 2020 - which marked the end of the first wave of SARS-CoV-2 infections in the  
413 UK - most of the initially recruited participants were infected prior to study enrolment and evaluated  
414 in the convalescent phase. Even with the contribution of acutely infected patients recruited chiefly  
415 during the second wave, this analysis mainly assesses the immune protective response and its  
416 durability. Finally, some of the sub-group analyses are likely to be underpowered to robustly detect  
417 differences in immune response.

418 In summary, our data suggest that patients with solid malignancies are capable of  
419 developing humoral and cellular immunity against SARS-CoV-2, with NAb detectable for up to 11  
420 months. In line with others,<sup>11,12</sup> we found that patients with haematological malignancies had  
421 impaired humoral response, which was associated with malignancy type and anti-CD20 treatments,  
422 but was often linked to detectable SsT-cell responses. Finally, we found that neutralising activity  
423 against VOCs was reduced in samples from patients infected with WT SARS-CoV-2, which raises  
424 concerns about the effectiveness of naturally acquired immune responses against new SARS-CoV-2  
425 VOCs. Whether such response can be boosted by COVID-19 vaccines remains under investigation in  
426 the vaccine cohort of CAPTURE, including the currently predominant Delta VOC (companion paper  
427 Fender *et al.*).

## 428 **Methods**

### 429 **Study design**

430 CAPTURE (NCT03226886) is a prospective, longitudinal cohort study that commenced recruitment in  
431 May 2020 at the Royal Marsden NHS Foundation Trust. The study design has been previously  
432 published.<sup>14</sup> In brief, adult patients with current or history of invasive cancer are eligible for  
433 enrolment (**Figure 1A**). Inclusion criteria are intentionally broad, and patients are approached  
434 irrespective of cancer type, stage, or treatment. Patients with confirmed or suspected SARS-CoV-2  
435 infection are targeted with broader recruitment in the course of routine clinical care (asymptomatic  
436 cases). Patients are screened at each study visit and classified as SARS-CoV-2-negative or SARS-CoV-  
437 2-positive based on a laboratory case definition of RT-PCR positive result and/or S1-reactive  
438 antibodies (details below). The primary endpoint is to describe the population characteristics of  
439 SARS-CoV-2 positive and negative cancer patients. The secondary endpoints include the impact of  
440 COVID-19 on long-term survival and ICU admission rates. Exploratory endpoints pertain to  
441 characterising clinical and immunological determinants of COVID-19 in cancer patients.

442

443 CAPTURE was approved as a substudy of TRACERx Renal (NCT03226886). TRACERx Renal was initially  
444 approved by the NRES Committee London, Fulham, on January 17, 2012. The TRACERx Renal sub-  
445 study CAPTURE was submitted as part of Substantial Amendment 9 and approved by the Health  
446 Research Authority on April 30, 2020 and the NRES Committee London - Fulham on May 1, 2020.  
447 CAPTURE is being conducted in accordance with the ethical principles of the Declaration of Helsinki,  
448 Good Clinical Practice and applicable regulatory requirements. All patients provided written  
449 informed consent to participate.

450

### 451 **Study schedule and follow-up**

452 Clinical data and sample collection for participating cancer patients is performed at baseline, and at  
453 clinical visits per standard-of-care management during the first year of follow-up; frequency varies  
454 depending on in- or outpatient status and systemic anti-cancer treatment regimens. For inpatients,  
455 study assessments are repeated every 2-14 days. For outpatients, the follow-up study assessments  
456 are aligned with clinically indicated hospital attendances. The frequency of study assessments in the  
457 first year for patients on anti-cancer therapies are as follows: every cycle for immune checkpoint  
458 inhibitors or targeted therapies; every second cycle for chemotherapy; every outpatient  
459 appointment (maximum 6 weekly) for patients on endocrine therapy or in surveillance or routine  
460 cancer care follow-up. Patient reported data is collected 3-monthly via an online questionnaire. In

461 year two to five of follow-up, the frequency of study assessments is reduced (see **Supplementary**  
462 **Material Study Protocol**).

### 463 **Data and Sample Sources**

464 Patient-reported outcome data are collected using PROFILES (Patient Reported Outcomes Following  
465 Initial treatment and Long-term evaluation of Survivorship; <https://profiles-study.rmh.nhs.uk/>).  
466 PROFILES is a web-based questionnaire administration and management system designed for the  
467 study of the physical and psychosocial impact of cancer and its treatment. Online questionnaires for  
468 baseline and follow up assessments were designed to record data for cancer patients participating in  
469 CAPTURE. Collected self-reported data include: ethnicity, smoking status, alcohol consumption,  
470 recent travel history, occupation, exercise habits, dietary habits, previous medical history,  
471 autoimmune disease (self, next of kin), vaccination history, concomitant medication, self-shielding  
472 status, previous SARS-CoV-2 tests, SARS-CoV-2 tests in household members, current and recent  
473 symptoms. Further demographic, epidemiological and clinical data (e.g. cancer type, cancer stage,  
474 treatment history) are collected from the internal electronic patient record system and entered into  
475 detailed case report forms in a secure electronic database. For information on anti-cancer  
476 intervention and response to most recent anti-cancer intervention, data was collected reflective of  
477 the time of SARS-CoV-2 infection per definition above where available, or the time of enrolment if  
478 data of disease onset is unknown (e.g. asymptomatic infections defined by positive serological  
479 positivity but negative/no RT-PCR results).

480 Study samples collected comprise blood samples, oropharyngeal swabs and archival and excess  
481 material from routine clinical investigations. Detailed sampling schedule and methodology has been  
482 previously described.<sup>14</sup> Surplus serum from patient biochemistry samples taken as part of routine  
483 care were also retrieved and linked to the study IDs before anonymisation and study analysis.  
484 Collected data and study samples are de-identified and stored with only the study-specific study  
485 identification number. For self-reported data, a PROFILES member number is used, which is  
486 generated automatically.

### 487 **WHO classification of severity of COVID-19**

488 We classified severity of COVID-19 according to the WHO clinical progression scale.<sup>47</sup> Uninfected:  
489 uninfected, no viral RNA detected - 0; Asymptomatic: viral RNA and/or S1-reactive IgG detected – 1;  
490 mild (ambulatory): symptomatic, independent – 2; symptomatic, assistance needed - 3; moderate  
491 (hospitalised): no oxygen therapy (if hospitalised for isolation only, record status as for ambulatory  
492 patient) – 4; oxygen by mask or nasal prongs - 5; severe (hospitalised): oxygen by non-invasive  
493 ventilation or high flow – 6; intubation and mechanical ventilation, pO<sub>2</sub>/FiO<sub>2</sub> ≥ 150 or SpO<sub>2</sub>/FiO<sub>2</sub> ≥

494 200 – 7; mechanical ventilation, pO<sub>2</sub>/FiO<sub>2</sub> < 150 (SpO<sub>2</sub>/FiO<sub>2</sub> < 200) or vasopressors – 8; mechanical  
495 ventilation, pO<sub>2</sub>/FiO<sub>2</sub> < 150 and vasopressors, dialysis, or extracorporeal membrane oxygenation - 9;  
496 Dead - 10.

#### 497 **Cell lines and viruses**

498 SUP-T1 cells stably transfected with spike or control vectors were obtained from M.P., and L.M.i.  
499 Vero E6 cells were from the National Institute for Biological Standards and Control, UK. The SARS-  
500 CoV-2 isolate hCoV-19/England/02/2020 was obtained from the Respiratory Virus Unit, Public Health  
501 England, UK, and propagated in Vero E6 cells.

#### 502 **Handling of oronasopharyngeal swabs, RNA isolation and RT-PCR**

503 SARS-CoV-2 RT-PCR was performed from oronasopharyngeal (ONP) swabs using a diagnostics assay  
504 established at the Francis Crick Institute. The complete standard operating procedure is available on  
505 the Crick Covid-19 consortium website: [https://www.crick.ac.uk/research/covid-19/covid19-](https://www.crick.ac.uk/research/covid-19/covid19-consortium)  
506 [consortium](https://www.crick.ac.uk/research/covid-19/covid19-consortium). ONP swabs were collected in VTM medium, frozen within 24 hrs after collection, and  
507 stored at -80°C until processing. ONP swabs were handled in a CL3 laboratory inside a biosafety  
508 cabinet using appropriate personal protective equipment and safety measures, which were in  
509 accordance with a risk assessment and standard operating procedure approved by the safety, health  
510 and sustainability committee at the Francis Crick Institute. In brief, 100 µl of swab vial content was  
511 inactivated in 5 M Guanidinium thiocyanate and RNA isolated using a completely automated kit-free,  
512 silica bead-based method.

513 PCR detection of SARS-CoV-2 was performed from 10 µl extracted RNA using two kits depending on  
514 the date of test. Up to 6<sup>th</sup> December 2020, samples were tested in duplicate using Real-Time  
515 Fluorescent RT-PCR Kit for Detecting 2019-nCoV (BGI). Positive, negative, and extraction controls  
516 were included on each plate. Runs were regarded as valid when negative control Ct values were >37  
517 and positive controls when Ct values were <37. Samples were only considered positive if Ct values in  
518 both replicates were <37. From 7<sup>th</sup> December 2020, tests were performed using TaqPath COVID-19  
519 CE-IVD RT-PCR Kit (Thermo Fisher), this time without replicate. Positive and negative controls were  
520 included on each plate and samples reported positive if 2 or 3 SARS-CoV-2 targets had Ct value <37  
521 and the internal control Ct <32. With both kits, samples with non-exponential amplification were  
522 excluded from analysis.

#### 523 **Viral Sequencing**

524 All PCR-positive samples with ORF1ab Ct value < 32 were selected for viral sequencing, representing  
525 52 samples from 32 patients. Sequencing was performed either on Illumina or on Oxford Nanopore

526 Technologies instruments. Oxford Nanopore libraries were prepared following the ARTIC nCoV-2019  
527 sequencing protocol v3 (LoCost) (protocols.io[https://protocols.io/view/ncov-2019-sequencing-  
528 protocol-v3-locost-bh42j8ye](https://protocols.io/view/ncov-2019-sequencing-protocol-v3-locost-bh42j8ye)) and then sequenced for 20 hours on a MinION flowcell on a GridION  
529 instrument. The ncov2019-artic-nf pipeline (version v1.1.1; [https://github.com/connor-  
530 lab/ncov2019-artic-nf](https://github.com/connor-lab/ncov2019-artic-nf)) written in the Nextflow domain specific language (version 20.10.0)<sup>48</sup> was used  
531 to perform the QC, variant calling and consensus sequence generation for the samples. The full  
532 command used was "nextflow run ncov2019-artic-nf --nanopolish --prefix \$PREFIX --basecalled\_fastq  
533 fastq\_pass/ --fast5\_pass fast5\_pass/ --sequencing\_summary sequencing\_summary.txt --  
534 schemeVersion V3 --minReadsPerBarcode 1 --minReadsArticGuppyPlex 1 -with-singularity artic-  
535 ncov2019-nanopore.img -profile singularity,slurm -r v1.1.1". Illumina libraries were prepared  
536 following the CoronaHiT protocol with minor modifications<sup>49</sup>, pooled and then sequenced at 100bp  
537 paired end on HiSeq 4000. The nf-core/viralrecon pipeline (version 1.1.0)<sup>50</sup> was used to perform the  
538 QC, variant calling and consensus sequence generation for the samples. The full command used was  
539 "nextflow run nf-core/viralrecon --input samplesheet.csv --genome 'MN908947.3' --amplicon\_bed  
540 nCoV-2019.artic.V3.bed --protocol 'amplicon' --callers ivar --skip\_assembly --skip\_markduplicates --  
541 skip\_fastqc --skip\_picard\_metrics --save\_align\_intermeds -profile crick -r 1.1.0". 44/52 passed  
542 quality control (>50% consensus sequence) and lineage was obtained using PANGOLIN  
543 (<https://github.com/cov-lineages/pangolin>). In the absence of sequencing data to confirm the  
544 causative SARS-CoV-2 variant, all patients tested with ThermoFisher TaqPath RT-PCR kit that  
545 reported S-dropout were considered to be infected with Alpha VOC.

#### 546 **Viral shedding**

547 Duration of viral shedding was estimated from research and opportunistic swabs and was defined as  
548 the time from first positive swab to the last positive swab (preceded by at least one negative swab).

#### 549 **Handling of whole blood samples**

550 All blood samples and isolated products were handled in a CL2 laboratory inside a biosafety cabinet  
551 using appropriate personal protective equipment and safety measures, which were in accordance  
552 with a risk assessment and standard operating procedure approved by the safety, health and  
553 sustainability committee of the Francis Crick Institute. For indicated experiments, serum or plasma  
554 samples were heat-inactivated at 56°C for 30 minutes prior to use after which they were used in a  
555 CL1 laboratory.

#### 556 **Plasma and PBMC isolation**

557 Whole blood was collected in EDTA tubes (VWR) and stored at 4°C until processing. All samples were  
558 processed within 24 hours. Time of blood draw, processing, and freezing was recorded for each  
559 sample. Prior to processing tubes were brought to room temperature (RT). PBMC and plasma were  
560 isolated by density-gradient centrifugation using pre-filled centrifugation tubes (pluriSelect). Up to  
561 30 ml of undiluted blood was added on top of the sponge and centrifuged for 30 minutes at 1000g at  
562 RT. Plasma was carefully removed then centrifuged for 10 minutes at 4000g to remove debris,  
563 aliquoted and stored at -80°C. The cell layer was then collected and washed twice in PBS by  
564 centrifugation for 10 minutes at 300 x g at RT. PBMC were resuspended in Recovery cell culture  
565 freezing medium (Fisher Scientific) containing 10% DMSO, placed overnight in CoolCell freezing  
566 containers (Corning) at -80°C and then stored at -80°C.

#### 567 **Serum isolation**

568 Whole blood was collected in serum coagulation tubes (Vacuette CAT tubes, Greiner) for serum  
569 isolation and stored at 4°C until processing. All samples were processed within 24 hrs. Time of blood  
570 draw, processing, and freezing was recorded for each sample. Tubes were centrifuged for 10  
571 minutes at 2000 x g at 4°C. Serum was separated from the clotted portion, aliquoted and stored at -  
572 80°C.

#### 573 **S1-reactive IgG ELISA**

574 Ninety-six-well MaxiSorp plates (Thermo Fisher Scientific) were coated overnight at 4°C with purified  
575 S1 protein in PBS (3 µg/ml per well in 50 µl) and blocked for 1 hour in blocking buffer (PBS, 5% milk,  
576 0.05% Tween 20, and 0.01% sodium azide). Sera were diluted in blocking buffer (1:50). Fifty  
577 microliters of serum were added to the wells and incubated for 2 hours at RT. After washing  
578 four times with PBS-T (PBS, 0.05% Tween 20), plates were incubated with alkaline phosphatase-  
579 conjugated goat anti-human IgG (1:1000, Jackson ImmunoResearch) for 1 hour. Plates were  
580 developed by adding 50 µl alkaline phosphatase substrate (Sigma Aldrich) for 15-30 minutes after six  
581 washes with PBS-T. Optical densities were measured at 405 nm on a microplate reader (Tecan).  
582 CR3022 (Absolute Antibodies) was used as a positive control. The cut-off for a positive response was  
583 defined as the mean negative value multiplied by 0.35 times the mean positive value.

#### 584 **Flow cytometry for spike-reactive IgG, IgM, and IgA**

585 SUP-T1 cells were harvested, counted and spike-expressing and control SUP-T1 cells were mixed in a  
586 1:1 ratio. The cell mix was transferred into V-bottom 96-well plates at 20,000 cells per well. Cells  
587 were incubated with heat-inactivated sera diluted 1:50 in PBS for 30 minutes, washed with FACS  
588 buffer (PBS, 5% BSA, 0.05% sodium azide), and stained with FITC anti-IgG (clone HP6017, Biolegend),

589 APC anti-IgM (clone MHM-88, Biolegend) and PE anti-IgA (clone IS11-8E10, Miltenyi Biotech) for 30  
590 minutes (all antibodies diluted 1:200 in FACS buffer). Cells were washed with FACS buffer and fixed  
591 for 20 minutes in 1% PFA in FACS buffer. Samples were run on a Bio-Rad Ze5 analyser running Bio-  
592 Rad Everest software v2.4 and analysed using FlowJo v10.7.1 (Tree Star Inc.) analysis software.  
593 Spike-expressing and control SUP-T1 cells were gated and mean fluorescence intensity (MFI) of both  
594 populations was measured. MFI in control SUP-T1 cells was subtracted from MFI in spike-expressing  
595 SUP-T1 cells, and resulting values were divided by MFI in control SUP-T1 cells to calculate the  
596 specific increase in MFI. Values >2 were considered positive.

#### 597 **Neutralising antibody assay against SARS-CoV-2**

598 Confluent monolayers of Vero E6 cells were incubated with SARS-CoV-2 WT or Alpha virus and two-  
599 fold serial dilutions of heat-treated serum or plasma samples starting at 1:40 for 4 hrs at 37°C, 5%  
600 CO<sub>2</sub>, in duplicates. The inoculum was then removed and cells were overlaid with viral growth  
601 medium. Cells were incubated at 37°C, 5% CO<sub>2</sub>. At 24 hours post-infection, cells were fixed in 4%  
602 paraformaldehyde and permeabilized with 0.2% Triton X-100/PBS. Virus plaques were visualized by  
603 immunostaining, as described previously for the neutralisation of influenza viruses using a rabbit  
604 polyclonal anti-NSP8 antibody used at 1:1000 dilution and anti-rabbit-HRP conjugated antibody at  
605 1:1000 dilution and detected by action of HRP on a tetramethyl benzidine-based substrate. Virus  
606 plaques were quantified and ID<sub>50</sub> was calculated.

#### 607 **High-throughput live virus microneutralisation assay**

608 High-throughput live virus microneutralisation assays were performed for a subset of 37 patients for  
609 WT SARS-CoV-2, Alpha, Beta or Delta. High-throughput live virus microneutralisation assays were  
610 performed as described previously.<sup>51</sup> Briefly, Vero E6 cells (Institute Pasteur) or Vero E6 cells  
611 expressing ACE2 and TMPRSS2 (VAT-1) (Centre for Virus Research)<sup>52</sup> at 90-100% confluency in 384-  
612 well format were first titrated with varying MOI of each SARS-CoV-2 variant and varying  
613 concentrations of a control monoclonal nanobody in order to normalise for possible replicative  
614 differences between variants and select conditions equivalent to wild-type virus. Following this  
615 calibration, cells were infected in the presence of serial dilutions of patient serum samples. After  
616 infection (24 hrs Vero E6 Pasteur, 16hrs VAT-1), cells were fixed with 4% final Formaldehyde,  
617 permeabilised with 0.2% TritonX-100, 3% BSA in PBS (v/v), and stained for SARS-CoV-2 N protein  
618 using Alexa488-labelled-CR3009 antibody produced in-house and cellular DNA using DAPI7. Whole-  
619 well imaging at 5x was carried out using an Opera Phenix (Perkin Elmer) and fluorescent areas and  
620 intensity calculated using the Phenix-associated software Harmony 9 (Perkin Elmer). Inhibition was  
621 estimated from the measured area of infected cells/total area occupied by all cells. The inhibitory

622 profile of each serum sample was estimated by fitting a 4-parameter dose response curve executed  
623 in SciPy. Neutralising antibody titres are reported as the fold-dilution of serum required to inhibit  
624 50% of viral replication (IC<sub>50</sub>), and are further annotated if they lie above the quantitative (complete  
625 inhibition) range, below the quantitative range but still within the qualitative range (i.e. partial  
626 inhibition is observed but a dose- response curve cannot be fit because it does not sufficiently span  
627 the IC<sub>50</sub>), or if they show no inhibition at all. IC<sub>50</sub> values above the quantitative limit of detection of  
628 the assay (>25600) were recoded as 3000; IC<sub>50</sub> values below the quantitative limit of the assay (< 40)  
629 but within the qualitative range were recoded as 39 and data below the qualitative range (i.e. no  
630 response observed) were recoded as 35.

### 631 **PBMC stimulation assay**

632 PBMC for in vitro stimulation were thawed at 37 °C and resuspended in 10 ml of warm complete  
633 medium (RPMI, 5% human AB serum) containing 0.02% benzonase. Viable cells were counted and  
634 1x10<sup>6</sup> to 2x10<sup>6</sup> cells were seeded in 200 µl complete medium per well of a 96-well plate. Cells were  
635 stimulated with 4 µl/well PepTivator SARS-CoV-2 spike (S), membrane (M), or nucleocapsid (N) pools  
636 (i.e., synthetic SARS-CoV-2 peptide pools, consisting of 15-mer sequences with 11 amino acid  
637 overlap covering the immunodominant parts of the S protein and the complete sequence of the N  
638 and membrane M proteins), representing 1µg/ml final concentration per peptide (Miltenyi Biotec,  
639 Surrey, UK). Staphylococcal enterotoxin B (Merck, UK) was used as a positive control at 0.5µg/ml  
640 final concentration, negative control was PBS containing DMSO at 0.002% final concentration. PBMC  
641 were cultured for 24 hrs at 37°C, 5% CO<sub>2</sub>.

### 642 **Activation-induced marker assay**

643 PBMC supernatants were collected for cytokine analysis after stimulation for 24 hours. Cells were  
644 washed twice in warm PBMC. Dead cells were stained with 0.5 µl/well Zombie dye V500 for 15  
645 minutes at RT in the dark, then washed once with PBS containing 2% FCS (FACS buffer). A surface  
646 staining mix was prepared per well, containing 2 µl/well of each antibody for surface staining (see  
647 **key resources table** for a full list of antibodies) in 50:50 brilliant stain buffer (BD) and FACS buffer.  
648 PBMC were stained with 50 µl surface staining mix per well for 30 minutes at RT in the dark. Cells  
649 were washed once in FACS buffer and fixed in 1% PFA in FACS buffer for 20 min, then washed once  
650 and resuspended in 200 µl PBS. All samples were acquired on a Bio-Rad Ze5 flow cytometer running  
651 Bio-Rad Everest software v2.4 and analysed using FlowJo v10.7.1 (Tree Star Inc.) analysis software.  
652 Compensation was performed with 20 µl antibody-stained anti-mouse Ig, k / negative control  
653 compensation particle set (BD Biosciences, UK). 1x10<sup>6</sup> live CD19-/CD14- cells were acquired per  
654 sample. Gates were drawn relative to the unstimulated control for each donor. T-cell response is



655 displayed as a stimulation index by dividing the percentage of AIM-positive cells by the percentage  
656 of cells in the negative control. If negative control was 0 the minimum value across the cohort was  
657 used. When S, M, and N stimulation were combined the sum of AIM-positive cells was divided by  
658 three times the percentage of positive cells in the negative control. A 1.5-fold increase in stimulation  
659 index is considered positive.

#### 660 **IFN- $\gamma$ ELISA**

661 IFN- $\gamma$  ELISA was performed using the human IFN- $\gamma$  DuoSet ELISA (R&D Systems) according to the  
662 manufacturer's instructions. Briefly, 96-well plates were coated overnight with capture antibody,  
663 washed twice in wash buffer then blocked with reagent diluent for 2 hrs at RT. 100  $\mu$ l of PBMC  
664 culture supernatants were added and incubated for 1 hr at RT and washed twice in wash buffer. 100  
665  $\mu$ l detection antibody diluted in reagent diluent was added per well and incubated for 2 hrs at RT.  
666 Plates were washed twice in wash buffer. 100  $\mu$ l streptavidin-HRP dilution was added to the plates  
667 and incubated for 20 minutes in the dark at RT, plates were washed twice in wash buffer. The  
668 reaction was developed using 200  $\mu$ l substrate solution for 20 minutes in the dark at RT then  
669 stopped with 50  $\mu$ l stop solution. Optical density was measured at 450 nm on a multimode  
670 microplate reader (Berthold). Serial dilutions of standard were run on each plate. Concentrations  
671 were calculated by linear regression of standard concentrations ranging 0-600 pg/ml and normalized  
672 to the number of stimulated PBMC. The assay sensitivity was 5 pg/ml.

#### 673 **Multiplex immune assay for cytokines and chemokines**

674 The preconfigured multiplex Human Immune Monitoring 65-plex ProcartaPlex immunoassay kit  
675 (Invitrogen, Thermo Fisher Scientific, UK) was used to measure 65 protein targets in plasma on the  
676 Bio-Plex platform (Bio-Rad Laboratories, Hercules, CA, USA), using Luminex xMAP technology.  
677 Analytes measured included APRIL; BAFF; BLC; CD30; CD40L; ENA-78; Eotaxin; Eotaxin-2; Eotaxin-3;  
678 FGF-2; Fractalkine; G-CSF; GM-CSF; Gro-Alpha; HGF; IFN-Alpha; IFN-gamma; IL-10; IL-12p70; IL-13; IL-  
679 15; IL-16; IL-17A; IL-18; IL-1Alpha; IL-1Beta; IL-2; IL-20; IL-21; IL-22; IL-23; IL-27; IL-2R; IL-3; IL-31; IL-4;  
680 IL-5; IL-6; IL-7; IL-8; IL-9; IP-10; I-TAC; LIF; MCP-1; MCP-2; MCP-3; M-CSF; MDC; MIF; MIG; MIP-  
681 1Alpha; MIP-1Beta; MIP-3Alpha; MMP-1; NGF-Beta; SCF; SDF-1Alpha; TNF-Beta; TNF-Alpha; TNF-R2;  
682 TRAIL; TSLP; TWEAK; VEGF-A. All assays were conducted as per the manufacturer's  
683 recommendation.

#### 684 **Statistics & Reproducibility**

685 No statistical method was used to predetermine sample size but as many patients with SARS-CoV-2  
686 infection were recruited as possible including patients with no history of infection to identify

687 patients in routine care with asymptomatic infection. The experiments were not randomised. The  
688 investigators were not blinded to allocation during experiments and outcome assessment.

689 Data and statistical analysis were done in FlowJo 10 and R v3.6.1 in R studio v1.2.1335. Gaussian  
690 distribution of baseline characteristics was tested by Kolmogorov-Smirnov test and differences in  
691 patient groups were compared using Chi-squared test, Mann-Whitney or Kruskal-Wallis tests as  
692 appropriate. Statistical methods for each experiment are provided in the figure legends. Gaussian  
693 distribution was tested by Kolmogorov-Smirnov test. Mann-Whitney, Wilcoxon, Kruskal-Wallis, Chi<sup>2</sup>,  
694 Fisher's exact test, and Friedman tests were performed for statistical significance. A p-value <0.05  
695 was considered significant. The ggplot2 package in R was used for data visualization and illustrative  
696 figures were created with BioRender.com. Data are usually plotted as single data points and box  
697 plots on a logarithmic scale. For boxplots, boxes represent upper and lower quartiles, line represents  
698 median, and whiskers IQR times 1.5. Notches represent confidence intervals of the median. For  
699 correlation matrix analysis, spearman rank correlation coefficients were calculated between all  
700 parameter pairs using the corplot package in R without clustering. For pairwise correlation  
701 spearman rank correlation coefficients were calculated. Multivariate binary logistic regression  
702 analysis was performed using the glm function with the stats package in R.

### 703 **Reporting Summary**

704 Further information on research design is available in the Nature Research Reporting Summary  
705 linked to this article.

### 706 **Data availability**

707 All requests for raw and analysed data, and CAPTURE study protocol will be reviewed by the  
708 CAPTURE Trial Management Team, Skin and Renal Clinical Trials Unit, The Royal Marsden NHS  
709 Foundation Trust ([CAPTURE@rmh.nhs.uk](mailto:CAPTURE@rmh.nhs.uk)) to determine if the request is subject to confidentiality  
710 and data protection obligations. Materials used in this study will be made available upon request.  
711 There are restrictions to the availability based on limited quantities. Response to any request for  
712 data and/or materials will be given within a 28 day period. Data and materials that can be shared  
713 would then be released upon completion of a material transfer agreement.

## 714 **Code availability**

715 No unpublished code was used in this study.

## 716 **Acknowledgements**

717 We thank the CAPTURE trial team, including Eleanor Carlyle, Kim Edmonds, and Lyra Del Rosario, as  
718 well as Somya Agarwal, Hamid Ahmod, Natalie Ash, Ravinder Dhaliwal, Lauren Dowdie, Tara Foley,  
719 Lucy Holt, Dilruba Kabir, Molly O’Flaherty, Mandisa Ndlovu, Sonia Ali, Justine Korteweg, Charlotte  
720 Lewis, Karla Lingard, Mary Mangwende, Aida Murra, Kema Peat, Sarah Sarker, Nahid Shaikh, Sarah  
721 Vaughan, and Fiona Williams. We acknowledge the tremendous support from the clinical and  
722 research teams at participating units at the Royal Marsden Hospital, including Ethel Black, Arnold  
723 Dela Rosa, Carole Pearce, Jessica Bazin, Leonora Conneely, Chloe Burrows, Tommy Brown, Jeremy  
724 Tai, Emma Lidington, Holly Hogan, Amanda Upadhyay, David Capdeferro, Ingrid Potyka, Annette  
725 Drescher, Farzana Baksh, Melissa Balcorta, Catia Da Costa Mendes, Joao Amorim, Venus Orejudos,  
726 and Louise Davison. We also thank the Volunteer Staff at The Francis Crick Institute, the Crick  
727 COVID19 consortium, Alice Lilley for help with neutralising assays, Antonia Toncheva, and the  
728 cloning unit at Autolus including James Sillibourne, Katarzyna Ward, Katarina Lamb and Philip Wu.  
729 We thank Brigitta Stockinger for her thoughtful review and comments on the manuscript. Due to the  
730 pace at which the field is evolving, we acknowledge researchers in COVID-19, particularly in  
731 furthering our understanding of SARS-CoV-2 infection and we apologise for work that was not cited.  
732 This research was funded in part, by the Cancer Research UK (grant reference number  
733 C50947/A18176). This work was supported by the Francis Crick Institute, which receives its core  
734 funding from Cancer Research UK (CRUK) (FC001988, FC001218, FC001099, FC001002, FC001078,  
735 FC001169, FC001030), the UK Medical Research Council (FC001988, FC001218, FC001099,  
736 FC001002, FC001078, FC001169, FC001030), and the Wellcome Trust (FC001988, FC001218,  
737 FC001099, FC001002, FC001078, FC001169, FC001030). For the purpose of Open Access, the author  
738 has applied a CC BY public copyright licence to any Author Accepted Manuscript version arising from  
739 this submission. TRACERx Renal is partly funded by the National Institute for Health Research (NIHR)  
740 Biomedical Research Centre (BRC) at the Royal Marsden Hospital and Institute of Cancer Research  
741 (ICR) (A109). The CAPTURE study is sponsored by The Royal Marsden NHS Foundation Trust and  
742 funded from a grant from The Royal Marsden Cancer Charity. A.F. has received funding from the  
743 European Union’s Horizon 2020 research and innovation programme under the Marie Skłodowska-  
744 Curie grant agreement No. 892360. L.A. is funded by the Royal Marsden Cancer Charity. S.T. is  
745 funded by Cancer Research UK (grant reference number A29911); the Francis Crick Institute, which  
746 receives its core funding from Cancer Research UK (FC10988), the UK Medical Research Council

747 (FC10988), and the Wellcome Trust (FC10988); the National Institute for Health Research (NIHR)  
748 Biomedical Research Centre at the Royal Marsden Hospital and Institute of Cancer Research (grant  
749 reference number A109), the Royal Marsden Cancer Charity, The Rosetrees Trust (grant reference  
750 number A2204), Ventana Medical Systems Inc (grant reference numbers 10467 and 10530), the  
751 National Institute of Health ((U01 CA247439) and Melanoma Research Alliance (Award Ref no  
752 686061). C.S. is Royal Society Napier Research Professor (RP150154). His work is supported by the  
753 Francis Crick Institute, which receives its core funding from Cancer Research UK (FC001169), the UK  
754 Medical Research Council (FC001169), and the Wellcome Trust (FC001169). C.S. is funded by Cancer  
755 Research UK (TRACERx, PEACE and CRUK Cancer Immunotherapy Catalyst Network), Cancer  
756 Research UK Lung Cancer Centre of Excellence, the Rosetrees Trust, Butterfield and Stoneygate  
757 Trusts, NovoNordisk Foundation (ID16584), Royal Society Research Professorship Enhancement  
758 Award (RP/EA/180007), the NIHR BRC at University College London Hospitals, the CRUK-UCL Centre,  
759 Experimental Cancer Medicine Centre and the Breast Cancer Research Foundation, USA (BCRF). His  
760 research is supported by a Stand Up To Cancer-LUNGevity-American Lung Association Lung Cancer  
761 Interception Dream Team Translational Research Grant (SU2C-AACR-DT23-17). Stand Up To Cancer  
762 is a program of the Entertainment Industry Foundation. Research grants are administered by the  
763 American Association for Cancer Research, the Scientific Partner of SU2C. C.S. also receives funding  
764 from the European Research Council (ERC) under the European Union's Seventh Framework  
765 Programme (FP7/2007-2013) Consolidator Grant (FP7-THESEUS-617844), European Commission ITN  
766 (FP7-PloidyNet 607722), an ERC Advanced Grant (PROTEUS) from the European Research Council  
767 under the European Union's Horizon 2020 research and innovation programme (835297) and  
768 Chromavision from the European Union's Horizon 2020 research and innovation programme  
769 (665233). R.W. has received Francis Crick Institute supported by Wellcome (FC0010218), UKRI  
770 (FC0010218), CRUK (FC0010218) and research funding from Wellcome (203135 and 222754),  
771 Rosetrees (M926) and The South African MRC.

## 772 **Author contributions**

773 Conceptualisation, S.T., L.A. and L.A.B.; Methodology, S.T., A.Fendler, F.B., K.A.W., G.K. and R.H.  
774 Software, M.G.; Formal Analysis, A.Fendler., L.A., S.T.C.S., G.K., K.W., R.W., R.H. and M.C.;  
775 Investigation, A.F., L.A., F.B., S.T.C.S, B.S., C.G., W.X., B.W., K.W., M.C., A.A-D. and R.H.; Resources,  
776 S.T., A.Fendler, L.A., L.A.B., F.B., S.T.C.S., B.S., C.G., B.W., W.X., M.C., G.C., M.P. and L.M., R.S., C.G.,  
777 H.F., M.G., F.G., O.C., T.S., Y.K., Z.T. and I.L.; Data Curation, L.A.B., S.T.C.S, B.S., C.G., A.Fendler and  
778 L.A.; Writing – Original Draft: S.T., K.R., A.Fendler, L.A., S.T.C.S.; Writing - Review & Editing: All;

779 Visualization, A.Fendler, S.T.C.S, S.T. and L.A.; Supervision, S.T.; Trial conduct, S.T., L.A., S.T.C.S, E.C.,  
780 L.R., K.E., L.A.B., J.L., N.Y., A.R., E.N. and S.K.

## 781 **Competing interests**

782 ST has received speaking fees from Roche, Astra Zeneca, Novartis and Ipsen. ST has the following  
783 patents filed: Indel mutations as a therapeutic target and predictive biomarker PCTGB2018/051892  
784 and PCTGB2018/051893 and Clear Cell Renal Cell Carcinoma Biomarkers P113326GB. N.Y. has  
785 received conference support from Celegene. A.R. received a speaker fee from Merck Sharp &  
786 Dohme. J.L. has received research funding from Bristol-Myers Squibb, Merck, Novartis, Pfizer,  
787 Achilles Therapeutics, Roche, Nektar Therapeutics, Covance, Immunocore, Pharmacyclics, and Aveo,  
788 and served as a consultant to Achilles, AstraZeneca, Boston Biomedical, Bristol-Myers Squibb, Eisai,  
789 EUSA Pharma, GlaxoSmithKline, Ipsen, Imugene, Incyte, iOnctura, Kymab, Merck Serono, Nektar,  
790 Novartis, Pierre Fabre, Pfizer, Roche Genentech, Secarna, and Vitaccess. I.C. has served as a  
791 consultant to Eli-Lilly, Bristol Meyers Squibb, MSD, Bayer, Roche, Merck-Serono, Five Prime  
792 Therapeutics, Astra-Zeneca, OncXerna, Pierre Fabre, Boehringer Ingelheim, Incyte, Astella, GSK,  
793 Sotio, Eisai and has received research funding from Eli-Lilly & Janssen-Cilag. He has received  
794 honorarium from Eli-Lilly, Eisai, Servier. A.O. acknowledges receipt of research funding from Pfizer  
795 and Roche; speakers fees from Pfizer, Seagen, Lilly and AstraZeneca; is an advisory board member of  
796 Roche, Seagen, and AstraZeneca; has received conference support from Leo Pharmaceuticals,  
797 AstraZeneca/Diachi-Sankyo and Lilly. C.S. acknowledges grant support from Pfizer, AstraZeneca,  
798 Bristol Myers Squibb, Roche-Ventana, Boehringer-Ingelheim, Archer Dx Inc (collaboration in minimal  
799 residual disease sequencing technologies) and Ono Pharmaceutical, is an AstraZeneca Advisory  
800 Board member and Chief Investigator for the MeRmaiD1 clinical trial, has consulted for Amgen,  
801 Pfizer, Novartis, GlaxoSmithKline, MSD, Bristol Myers Squibb, Celgene, AstraZeneca, Illumina,  
802 Genentech, Roche-Ventana, GRAIL, Medicxi, Metabomed, Bicycle Therapeutics, and the Sarah  
803 Cannon Research Institute, has stock options in Apogen Biotechnologies, Epic Bioscience, GRAIL, and  
804 has stock options and is co-founder of Achilles Therapeutics. Patents: C.S. holds European patents  
805 relating to assay technology to detect tumour recurrence (PCT/GB2017/053289); to targeting  
806 neoantigens (PCT/EP2016/059401), identifying patient response to immune checkpoint blockade  
807 (PCT/EP2016/071471), determining HLA LOH (PCT/GB2018/052004), predicting survival rates of  
808 patients with cancer (PCT/GB2020/050221), identifying patients who respond to cancer treatment  
809 (PCT/GB2018/051912), a US patent relating to detecting tumour mutations (PCT/US2017/28013)  
810 and both a European and US patent related to identifying insertion/deletion mutation targets  
811 (PCT/GB2018/051892). L.P. has received research funding from Pierre Fabre, and honoria from

812 Pfizer, Ipsen, Bristol-Myers Squibb, and EUSA Pharma. S.B. has received institutional research  
813 funding from Astrazeneca, Tesaro, GSK; speakers fees from Amgen, Pfizer, Astrazeneca, Tesaro, GSK,  
814 Clovis, Takeda, Immunogen, Mersana and has an advisor role for Amgen, Astrazeneca, Epsilogen,  
815 Genmab, Immunogen, Mersana, MSD, Merck Serono, Oncxerna, Pfizer, Roche. A.R. has received  
816 speaker's fee from Merck Sharp & Dohme. Remaining authors have no conflicts of interest to  
817 declare.

818

819

820

821 **Tables**822 **Table 1:** CAPTURE cohort overview

	<b>Cohort</b>	<b>SARS-CoV-2 infection</b>	<b>No SARS-CoV2 Infection</b>
<b>Cohort Characteristics</b>	n= 357	n= 118	n= 239
Age, years (median, range)	59 (18-87)	60 (18-87)	60 (26- 82)
Male, n (%)	192 (54)	64 (54)	128 (54)
<b>Cancer diagnosis, n (%)</b>			
Skin	79 (22)	10 (8)	69 (29)
Gastrointestinal	71 (20)	30 (25)	39 (16)
Urology	62 (17)	15 (12)	48 (20)
Lung	41 (11)	8 (7)	33 (14)
Haematological	39 (11)	21 (17)	17 (7)
Breast	31 (9)	16 (13)	16 (7)
Gynaecological	22 (6)	9 (7)	13 (5)
Sarcoma	12 (3)	4 (3)	8 (3)
Head & Neck	6 (2)	5 (4)	1 (0)
Other	4 (1)	4 (3)	0 (0)
<b>Cancer stage, n (%)</b>			
Stage I-II	20 (6)	7 (6)	13 (5)
Stage III	72 (20)	22 (18)	50 (22)
Stage IV	229 (64)	70 (58)	159 (67)
Haematological	39 (11)	21 (17)	17 (7)
<b>Days of Follow up, median (IQR)</b>	154 (63-273)	110 (58-274)	164 (63-274)

823

824 **Table 2.** Oncological and medical history of SARS-CoV-2 positive patients

<b>N=118</b>	
<b>Past medical history</b>	
HTN	31 (27)
PVD/IHD/CVD	9 (8)
Diabetes Mellitus	14 (11)
Obesity, BMI>30, n (%)	25 (21)
Inflammatory/Autoimmune	7 (6)
<b>Smoking status</b>	
Current smoker	36 (31)
Ex-smoker	51 (43)
Never smoked	12 (10)
Unknown	19 (16)
<b>Oncological history</b>	
<b>Solid tumours, n=97</b>	
Disease status (in respect to last treatment)	
<b>SACT, palliative, n=74</b>	
CR/PR	27 (28)
SD	24 (24)
PD	23 (24)
<b>SACT, neoadjuvant or radical CRT</b>	8 (8)
<b>Surgery ± adjuvant SACT</b>	15 (15)
<b>Treatment within 12 weeks</b>	
<b>Systemic therapy</b>	
Chemotherapy	43 (44)
Small molecule inhibitor	15 (15)
Anti-PD(L)1 ± anti-CTLA4	14 (14)
Endocrine therapy	7 (6)
No treatment	5 (4)



**Local therapy**

Surgery	15 (13)
Radiotherapy	11 (10)

---

**Haematological malignancies, n=21**


---

**Diagnosis**

Acute leukaemia	11 (52)
Lymphoma	6 (29)
Myeloma	4 (19)

**Disease status**

MRD/CR	5 (24)
Partial remission	7 (33)
SD	3 (14)
PD/relapse/untreated acute presentation	7 (33)

**Treatment within 12 weeks**

Chemotherapy	17 (81)
Targeted therapy	10 (48)
Anti-CD20 therapy	6 (29)
CAR-T	1 (5)

**Haematologic stem cell transplant**

Auto/Allograft pre-COVID-19	6 (29)
Auto/Allograft post-COVID-19	2 (9)

---

825

826 AS, active surveillance; BMI, body mass index; CAR-T, Chimeric antigen receptor T cell; CD-20, B-  
827 lymphocyte antigen; CR, complete response; CRT, chemoradiotherapy; CRP, C-reactive protein;  
828 CTLA-4, cytotoxic T-lymphocyte associated protein 4; DM, diabetes mellitus; GVHD, graft versus  
829 host disease; Hb, haemoglobin; HTN, hypertension; IHD, ischaemic heart disease; IQR, interquartile  
830 range; mAb, monoclonal antibody; MRD, minimal residual disease; NED, no evidence of disease; N0,  
831 neutrophil; PCR, polymerase chain reaction; PD progressive disease; PD(L)-1, program death (ligand)  
832 -1; Plt, platelet; PVD, peripheral vascular disease; SACT, systemic anti-cancer therapy; SD, stable  
833 disease; WBC, white cell blood count; WHO, world health organization

834

835

836

837

838 **Table 3:** Clinical characteristics of COVID-19 illness

<b>COVID-19 characteristics</b>	<b>n (%)</b>
<b>Viral shedding status</b>	
PCR positive, n (%)	95 (81)
Duration of PCR positivity, days median (range)	12 (6-80)
<b>WHO Severity Score</b>	
1, Asymptomatic	24 (20)
2-3, Mild	52 (44)
4-5, Moderate	36 (31)
>5, Severe	6 (5)
<b>Admission to hospital</b>	
Not hospitalised	54 (49)
Admitted with COVID-19- like illness	33 (29)
COVID-19 illness during hospitalisation	30 (25)
Duration of admission, days; median (range)	9 (1 – 120)
<b>Complications of COVID-19</b>	
Required supplemental oxygen	27 (23)
Pneumonia	29 (25)
Venous/arterial thromboembolism	9 (8)
Admission to ITU	7 (6)
Need for mechanical ventilation/NIV	4 (3)
<b>COVID-19 directed therapy</b>	
Corticosteroids	13 (11)
Anti-IL6 mAB	3 (3)
<b>Laboratory Investigations, median (IQR)</b>	
<b>Haematology</b>	
Hb, g/DL	110 (93 – 128)

WBC, x10 <sup>6</sup> /L	5.7 (3.4 – 8.0)
NO, x10 <sup>6</sup> /L	3.8 (2.1– 5.5)
Plt, x10 <sup>6</sup> /L	213 (130 – 299)
<b>Biochemistry</b>	
Creatinine, umol/L	60 (53 – 71)
CRP, mg/L	59 (23 – 134)
<b>Clinical outcomes and impact</b>	
<b>Survival</b>	
Deceased, n (%)	13 (10)
Death within 30 days of PCR positivity	4 (3)
<b>Primary cause death:</b>	
Progressive Cancer	11 (9)
Complications of COVID-19	2 (2)

839

840

CRP, C-reactive protein; Hb, haemoglobin; IL-6, interleukin-6; IQR, interquartile range; mAb, monoclonal antibody; NIV,

841

non-invasive ventilation; NO, neutrophil; PCR, polymerase chain reaction; Plt, platelet; WBC, white cell blood count; WHO,

842

World Health Organization;

843

844

845

846

847

848

849

850

851 **Figure legends**

852 **Figure 1: SARS-CoV-2 infection status, viral shedding, and COVID-19 symptoms of recruited**  
853 **patients.**

854 **a)** Patients with cancer irrespective of cancer type, stage, or treatment were recruited. Follow-up  
855 schedules for patients with cancer were bespoke to their COVID-19 status and account for their  
856 clinical schedules (inpatients: every 2 – 14 days; outpatients: every clinical visit maximum every 3-6  
857 weeks in year one and every six months in year two, and at the start of every or every-second cycle  
858 of treatment). Clinical data, oronasopharyngeal swabs and blood were collected at each study visit.  
859 Viral antigen testing (RT-PCR on swabs), antibody (ELISA, flow cytometric assay), T cell response and  
860 IFN- $\gamma$  activation assays were performed. **b)** Distribution of SARS-CoV-2 infection, and S1-reactive Ab  
861 status and COVID-19 severity in patients with cancer. 357 patients with cancer were recruited  
862 between May 4, 2020 and March 31st 2021. SARS-CoV-2 infection status by RT-PCR and S1-reactive  
863 Ab were analysed at recruitment and in serial samples. RT-PCR results prior to recruitment were  
864 extracted from electronic patient records. COVID-19 case definition includes all patients with either  
865 RT-PCR confirmed SARS-CoV-2 infection or S1-reactive Ab. **c)** Viral shedding in 43 patients with serial  
866 positive swabs. Solid bars indicate time to the last positive test, dotted lines denote the time from  
867 the last positive test to the first negative test. **d)** Distribution of symptoms in 118 COVID-19 patients.  
868 Bar graph denotes the number of patients. Each row in the lower graph denotes one patient. ONP,  
869 Oronasopharyngeal; ELISA, enzyme-linked immunoassay; PBMCs, peripheral blood mononuclear  
870 cells; WGS - whole genome sequencing, RTx, radiotherapy, HSCT, human stem cell transplant.

871

872 **Figure 2: S1-reactive and antibody response in patients with cancer**

873 **a)** S1-reactive AbT by COVID-19 severity (n=112 patients). Significance was tested by Kruskal-Wallis  
874 test,  $p = 0.074$ . **b)** S1-reactive AbT by cancer type (Solid patients: n= 92, Haematological patients:  
875 n=20). Significance was tested by two-sided Wilcoxon Wilcoxon-Mann-Whitney U test,  $p = 0.011$ . **c)**  
876 NAbT by COVID-19 severity (n=112 patients). Significance was tested by Kruskal-Wallis test,  $p =$   
877  $0.0027$ . **d)** NAbT by cancer type (Solid patient: n= 92, Haematological patients: n=20). Significance  
878 was tested by two-sided Wilcoxon-Mann-Whitney U test,  $p = 0.052$ . Boxes indicate 25 and 75  
879 percentiles, line indicates median, and whiskers indicate 1.5 times the IQR. Dots represent individual  
880 samples. Dotted lines and grey boxes denote the limit of detection. **e)** Multivariate binary logistic  
881 regression evaluating association with lack of NAb in patients with cancer (n=112). Wald z-statistic  
882 was used to calculate two-sided p-values. \*,  $p = 0.038$ . **f)** Multivariate binary logistic regression  
883 evaluating the association of lack of NAb in patients with solid cancer (n = 92). **g)** Multivariate binary

884 logistic regression evaluating the association of lack of NAb in patients with solid cancer (n = 92). Dot  
885 denotes odds ratio (blue, positive odds ratio; red, negative odds ratio); whiskers indicate 1.5 times  
886 the IQR. **h)** NAbT against WT, Alpha, Beta, and Delta VOCs in patients (n=112) infected with WT  
887 SARS-CoV-2 or Alpha VOC. Violin plots denote density of data points. PointRange denotes median  
888 and 25 and 75 percentiles. Dots represent individual samples. Significance was tested by Kruskal  
889 Wallis test,  $p = 3.5e-07$ , two-sided Wilcoxon Mann Whitney U-test with Bonferroni correction (post-  
890 hoc test) was used for pairwise comparisons. p-values are denoted in the graph. **i)** S1-reactive AbT  
891 and **j)** NAbT post onset of disease (n=97 patients). Blue line denotes loess regression line with 95%  
892 confidence bands in grey. Black dots denote patients with one sample, coloured dots denote  
893 patients with serial samples (n=51 patients). Samples from individual patients are connected. Dotted  
894 lines and grey areas at bottom indicate limit of detection. NAb, neutralising antibody, NAbT,  
895 neutralising antibody titres, AbT, Antibody titres.

896

### 897 **Figure 3: T cell response in patients with cancer**

898 **a,b)** Representative plots of  $CD4^+CD137^+OX40^+$  ( $CD4^+$ ) and  $CD8^+CD137^+CD69^+$  ( $CD8^+$ ) T cells in a  
899 patient with confirmed COVID-19 and a cancer patient without COVID-19 after in vitro stimulation  
900 with S, M, and N peptide pools, positive control (Staphylococcal enterotoxin B, SEB) or negative  
901 control (NC). Frequency of Sars-CoV-2-specific **c)**  $CD4^+$  and **d)**  $CD8^+$  T cells in solid patients with  
902 cancer (n= 83). Frequency of Sars-CoV-2-specific **e)**  $CD4^+$  and **f)**  $CD8^+$  T cells in haematological  
903 patients with cancer (n= 21). Stimulation index was calculated by dividing the percentage of positive  
904 cells in the stimulated sample by the percentage of positive cells in the negative control (NC). To  
905 obtain the total number of SsT cells the sum of cells activated by S, M, and N was calculated (SMN).  
906 Boxes indicate the 25 and 75 percentiles, line indicates the median, and whiskers indicate 1.5 times  
907 the IQR. Individual patients are represented as dots. Dots represent individual samples. Dotted lines  
908 and grey boxes denote the limit of detection. SsT cells, Sars-CoV-2-specific T cells.

909

910

### 911 **Figure 4: Comparison of antibody and T cell responses in patients with cancer**

912 **a)** S1-reactive AbT in patients with leukaemia (n=11), myeloma (n=4), and lymphoma (n=6). **b)**  
913 Neutralising antibody titres in patients with leukaemia (n=10), myeloma (n=4), and lymphoma (n=6).  
914 **c)**  $CD4^+$  and  $CD8^+$  cells T cells across patients with leukemia (n=10), myeloma (n=4), or lymphoma  
915 (n=6). Stimulation index was calculated by dividing the percentage of  $CD4^+CD137^+OX40^+$  ( $CD4^+$ ) and  
916  $CD8^+CD137^+CD69^+$  ( $CD8^+$ ) T cells in the stimulated sample by the percentage of positive cells in the  
917 negative control (NC). Significance was tested by Kruskal-Wallis test,  $p < 0.05$  was considered

918 significant. **d)** S1-reactive AbT in patients with haematological malignancy receiving anti-CD20  
919 treatment (n=6) vs other SACT (n=15). **e)** NAbT in patients with haematological malignancy receiving  
920 anti-CD20 treatment (n=6) vs other SACT (n=15). Significance was tested by two-sided Wilcoxon-  
921 Mann-Whitney U test,  $p < 0.05$  was considered significant. **f)** Comparison of CD4<sup>+</sup>/CD8<sup>+</sup> T cells  
922 between patients with haematological malignancies on anti-CD20 therapy (n=5, administered within  
923 six months) and not on anti-CD20 therapy (n=15). Significance was tested by two-sided Wilcoxon-  
924 Mann-Whitney U test,  $p < 0.05$  was considered significant. **g)** CD4<sup>+</sup> and CD8<sup>+</sup> cells T cells across  
925 patients with solid cancer (n=81) by cancer subtype. Boxes indicate the 25 and 75 percentiles, line  
926 indicates the median, and whiskers indicate 1.5 times the IQR. Dots represent individual patient  
927 samples. Dotted lines and grey boxes denote the limit of detection. Significance was tested by  
928 Kruskal-Wallis test,  $p < 0.05$  was considered significant. SACT, systemic anti-cancer therapy.

929

930 **Figure 5: Associations between SARS-CoV-2-specific T cells with patient or cancer-specific features**

931 Multivariate binary logistic regression analysis evaluating associations between SARS-CoV-2-specific  
932 **a)** CD4<sup>+</sup> and **b)** CD8<sup>+</sup> T cells with cancer diagnosis (solid vs haematological malignancies),  
933 comorbidities, age, sex, and COVID-19 disease severity in 100 patients. Wald z-statistic was used to  
934 calculate two-sided p-values. \*,  $p = 0.038$ . Multivariate binary logistic regression analysis evaluating  
935 associations between SARS-CoV-2-specific **c)** CD4<sup>+</sup> and **d)** CD8<sup>+</sup> T cells with anti-cancer intervention,  
936 age, sex, and COVID-19 disease severity in patients with solid cancer (n=81). Wald z-statistic was  
937 used to calculate two-sided p-values. \*,  $p = 0.045$ . Dot denotes odds ratio (blue and red dots  
938 indicate positive or negative odds ratio, respectively) ; whiskers indicate 1.5 times the IQR. **e)**  
939 Comparison of SARS-CoV-2-specific CD4<sup>+</sup>/CD8<sup>+</sup> T cells between patients with solid malignancies on  
940 CPI (n=13, administered within three months) and not on CPI (n=68). Boxes indicate the 25th and  
941 75th percentiles, line indicates the median, and whiskers indicate 1.5 times the IQR. Dots represent  
942 individual samples. Significance was tested by two-sided Wilcoxon-Mann-Whitney U test ( $p = 0.038$   
943 and 0.53).

944

945

946

947

948

949

950

951

952 **References**

- 953 1 Williamson, E. J. et al. Factors associated with COVID-19-related death using OpenSAFELY.  
954 *Nature* 584, 430-436, doi:10.1038/s41586-020-2521-4 (2020).
- 955 2 Saini, K. S. et al. Mortality in patients with cancer and coronavirus disease 2019: A  
956 systematic review and pooled analysis of 52 studies. *Eur J Cancer* **139**, 43-50,  
957 doi:10.1016/j.ejca.2020.08.011 (2020).
- 958 3 Garcia-Suarez, J. et al. Impact of hematologic malignancy and type of cancer therapy on  
959 COVID-19 severity and mortality: lessons from a large population-based registry study. *J Hematol*  
960 *Oncol* **13**, 133, doi:10.1186/s13045-020-00970-7 (2020).
- 961 4 Garassino, M. C. et al. COVID-19 in patients with thoracic malignancies (TERAVOLT): first  
962 results of an international, registry-based, cohort study. *Lancet Oncol* **21**, 914-922,  
963 doi:10.1016/S1470-2045(20)30314-4 (2020).
- 964 5 Lee, L. Y. et al. COVID-19 mortality in patients with cancer on chemotherapy or other  
965 anticancer treatments: a prospective cohort study. *Lancet* **395**, 1919-1926, doi:10.1016/S0140-  
966 6736(20)31173-9 (2020).
- 967 6 Kuderer, N. M. et al. Clinical impact of COVID-19 on patients with cancer (CCC19): a cohort  
968 study. *Lancet* **395**, 1907-1918, doi:10.1016/S0140-6736(20)31187-9 (2020).
- 969 7 Grivas, P. et al. Association of clinical factors and recent anticancer therapy with COVID-19  
970 severity among patients with cancer: a report from the COVID-19 and Cancer Consortium. *Ann Oncol*  
971 **32**, 787-800, doi:10.1016/j.annonc.2021.02.024 (2021).
- 972 8 Lee, L. Y. W. et al. COVID-19 prevalence and mortality in patients with cancer and the effect  
973 of primary tumour subtype and patient demographics: a prospective cohort study. *Lancet Oncol* **21**,  
974 1309-1316, doi:10.1016/s1470-2045(20)30442-3 (2020).
- 975 9 Crolley, V. E. et al. COVID-19 in cancer patients on systemic anti-cancer therapies: outcomes  
976 from the CAPITOL (COVID-19 Cancer PatienT Outcomes in North London) cohort study. *Ther Adv*  
977 *Med Oncol* **12**, 1758835920971147, doi:10.1177/1758835920971147 (2020).
- 978 10 Robilotti, E. V. et al. Determinants of COVID-19 disease severity in patients with cancer. *Nat*  
979 *Med*, doi:10.1038/s41591-020-0979-0 (2020).
- 980 11 Bange, E. M. et al. CD8(+) T cells contribute to survival in patients with COVID-19 and  
981 hematologic cancer. *Nat Med* **27**, 1280-1289, doi:10.1038/s41591-021-01386-7 (2021).
- 982 12 Abdul-Jawad, S. et al. Acute Immune Signatures and Their Legacies in Severe Acute  
983 Respiratory Syndrome Coronavirus-2 Infected Cancer Patients. *Cancer Cell* **39**, 257-275.e256,  
984 doi:10.1016/j.ccell.2021.01.001 (2021).

985 13 Thakkar, A. *et al.* Patterns of seroconversion for SARS-CoV-2 IgG in patients with malignant  
986 disease and association with anticancer therapy. *Nature Cancer* **2**, 392-399, doi:10.1038/s43018-  
987 021-00191-y (2021).

988 14 Au, L. *et al.* Cancer, COVID-19, and Antiviral Immunity: The CAPTURE Study. *Cell* **183**, 4-10,  
989 doi:10.1016/j.cell.2020.09.005 (2020).

990 15 A minimal common outcome measure set for COVID-19 clinical research. *Lancet Infect Dis*  
991 **20**, e192-e197, doi:10.1016/s1473-3099(20)30483-7 (2020).

992 16 Kuderer, N. M. *et al.* Clinical impact of COVID-19 on patients with cancer (CCC19): a cohort  
993 study. *Lancet* **395**, 1907-1918, doi:10.1016/s0140-6736(20)31187-9 (2020).

994 17 Lowe, K. E., Zein, J., Hatipoglu, U. & Attaway, A. Association of Smoking and Cumulative  
995 Pack-Year Exposure With COVID-19 Outcomes in the Cleveland Clinic COVID-19 Registry. *JAMA*  
996 *Intern Med* **181**, 709-711, doi:10.1001/jamainternmed.2020.8360 (2021).

997 18 Sterlin, D. *et al.* IgA dominates the early neutralizing antibody response to SARS-CoV-2. *Sci.*  
998 *Transl. Med.* **13**, eabd2223, doi:10.1126/scitranslmed.abd2223 (2021).

999 19 Grifoni, A. *et al.* Targets of T Cell Responses to SARS-CoV-2 Coronavirus in Humans with  
1000 COVID-19 Disease and Unexposed Individuals. *Cell*, doi:10.1016/j.cell.2020.05.015.

1001 20 Dan, J. M. *et al.* Immunological memory to SARS-CoV-2 assessed for up to 8 months after  
1002 infection. *Science* **371**, eabf4063, doi:10.1126/science.abf4063 (2021).

1003 21 Moderbacher, C. R. *et al.* Antigen-specific adaptive immunity to SARS-CoV-2 in acute COVID-  
1004 19 and associations with age and disease severity. *Cell*, doi:10.1016/j.cell.2020.09.038 (2020).

1005 22 Weiskopf, D. *et al.* Phenotype and kinetics of SARS-CoV-2-specific T cells in COVID-19  
1006 patients with acute respiratory distress syndrome. *Science immunology* **5**, eabd2071,  
1007 doi:10.1126/sciimmunol.abd2071 (2020).

1008 23 Crotty, S. T Follicular Helper Cell Biology: A Decade of Discovery and Diseases. *Immunity* **50**,  
1009 1132-1148, doi:<https://doi.org/10.1016/j.immuni.2019.04.011> (2019).

1010 24 Mateus, J. *et al.* Selective and cross-reactive SARS-CoV-2 T cell epitopes in unexposed  
1011 humans. *Science*, eabd3871, doi:10.1126/science.abd3871 (2020).

1012 25 Marra, A. *et al.* Seroconversion in patients with cancer and oncology health care workers  
1013 infected by SARS-CoV-2. *Ann Oncol* **32**, 113-119, doi:10.1016/j.annonc.2020.10.473 (2021).

1014 26 Earle, K. A. *et al.* Evidence for antibody as a protective correlate for COVID-19 vaccines.  
1015 *Vaccine* **39**, 4423-4428, doi:<https://doi.org/10.1016/j.vaccine.2021.05.063> (2021).

1016 27 Khoury, D. S. *et al.* Neutralizing antibody levels are highly predictive of immune protection  
1017 from symptomatic SARS-CoV-2 infection. *Nature Medicine* **27**, 1205-1211, doi:10.1038/s41591-021-  
1018 01377-8 (2021).



1019 28 Seow, J. *et al.* Longitudinal observation and decline of neutralizing antibody responses in the  
1020 three months following SARS-CoV-2 infection in humans. *Nature Microbiology* **5**, 1598-1607,  
1021 doi:10.1038/s41564-020-00813-8 (2020).

1022 29 Gaebler, C. *et al.* Evolution of antibody immunity to SARS-CoV-2. *Nature* **591**, 639-644,  
1023 doi:10.1038/s41586-021-03207-w (2021).

1024 30 Wang, Z. *et al.* Naturally enhanced neutralizing breadth against SARS-CoV-2 one year after  
1025 infection. *Nature* **595**, 426-431, doi:10.1038/s41586-021-03696-9 (2021).

1026 31 Achiron, A. *et al.* SARS-CoV-2 antibody dynamics and B-cell memory response over time in  
1027 COVID-19 convalescent subjects. *Clin Microbiol Infect*, doi:10.1016/j.cmi.2021.05.008 (2021).

1028 32 Vacharathit, V. *et al.* SARS-CoV-2 variants of concern exhibit reduced sensitivity to live-virus  
1029 neutralization in sera from CoronaVac vaccinees and naturally infected COVID-19 patients. medRxiv,  
1030 2021.2007.2010.21260232, doi:10.1101/2021.07.10.21260232 (2021).

1031 33 Juno, J. A. *et al.* Humoral and circulating follicular helper T cell responses in recovered  
1032 patients with COVID-19. *Nature Medicine* **26**, 1428-1434, doi:10.1038/s41591-020-0995-0 (2020).

1033 34 Murugesan, K. *et al.* Interferon-gamma release assay for accurate detection of SARS-CoV-2 T  
1034 cell response. *Clinical Infectious Diseases*, doi:10.1093/cid/ciaa1537 (2020).

1035 35 Pauken, K. E. *et al.* The PD-1 Pathway Regulates Development and Function of Memory  
1036 CD8<sup>+</sup> T Cells following Respiratory Viral Infection. *Cell Reports* **31**,  
1037 doi:10.1016/j.celrep.2020.107827 (2020).

1038 36 Konkel, J. E. *et al.* PD-1 signalling in CD4(+) T cells restrains their clonal expansion to an  
1039 immunogenic stimulus, but is not critically required for peptide-induced tolerance. *Immunology* **130**,  
1040 92-102, doi:10.1111/j.1365-2567.2009.03216.x (2010).

1041 37 Apostolidis, S. A. *et al.* Altered cellular and humoral immune responses following SARS-CoV-  
1042 2 mRNA vaccination in patients with multiple sclerosis on anti-CD20 therapy. medRxiv,  
1043 2021.2006.2023.21259389, doi:10.1101/2021.06.23.21259389 (2021).

1044 38 Zhao, J., Zhao, J. & Perlman, S. T cell responses are required for protection from clinical  
1045 disease and for virus clearance in severe acute respiratory syndrome coronavirus-infected mice. *J.*  
1046 *Virol.* **84**, 9318-9325, doi:10.1128/jvi.01049-10 (2010).

1047 39 Tan, A. T. *et al.* Early induction of functional SARS-CoV-2-specific T cells associates with rapid  
1048 viral clearance and mild disease in COVID-19 patients. *Cell Rep.* **34**, 108728,  
1049 doi:https://doi.org/10.1016/j.celrep.2021.108728 (2021).

1050 40 Muñoz-Fontela, C. *et al.* Animal models for COVID-19. *Nature* **586**, 509-515,  
1051 doi:10.1038/s41586-020-2787-6 (2020).

1052 41 Sahin, U. et al. COVID-19 vaccine BNT162b1 elicits human antibody and T(H)1 T cell  
1053 responses. *Nature* 586, 594-599, doi:10.1038/s41586-020-2814-7 (2020).

1054 42 Ewer, K. J. et al. T cell and antibody responses induced by a single dose of ChAdOx1 nCoV-19  
1055 (AZD1222) vaccine in a phase 1/2 clinical trial. *Nat. Med.* 27, 270-278, doi:10.1038/s41591-020-  
1056 01194-5 (2021).

1057 43 Tarke, A. et al. Impact of SARS-CoV-2 variants on the total CD4(+) and CD8(+) T cell reactivity  
1058 in infected or vaccinated individuals. *Cell Rep Med* 2, 100355, doi:10.1016/j.xcrm.2021.100355  
1059 (2021).

1060 44 Sekine, T. et al. Robust T Cell Immunity in Convalescent Individuals with Asymptomatic or  
1061 Mild COVID-19. *Cell* 183, 158-168.e114, doi:https://doi.org/10.1016/j.cell.2020.08.017 (2020).

1062 45 Le Bert, N. et al. SARS-CoV-2-specific T cell immunity in cases of COVID-19 and SARS, and  
1063 uninfected controls. *Nature* 584, 457-462, doi:10.1038/s41586-020-2550-z (2020).

1064 46 Angelis, V. *et al.* Defining the true impact of coronavirus disease 2019 in the at-risk  
1065 population of patients with cancer. *Eur J Cancer* **136**, 99-106, doi:10.1016/j.ejca.2020.06.027 (2020).

1066

1067

1068 **Methods-only references**

1069

1070 47 Aitken, J. et al. Scalable and robust SARS-CoV-2 testing in an academic center. Nat.  
1071 Biotechnol., doi:10.1038/s41587-020-0588-y (2020).

1072 48 Di Tommaso, P. et al. Nextflow enables reproducible computational workflows. Nat  
1073 Biotechnol 35, 316-319, doi:10.1038/nbt.3820 (2017).

1074 49 Baker, D. J. et al. CoronaHiT: high-throughput sequencing of SARS-CoV-2 genomes. Genome  
1075 Med. 13, 21, doi:10.1186/s13073-021-00839-5 (2021).

1076 50 Ewels, P. A. et al. The nf-core framework for community-curated bioinformatics pipelines.  
1077 Nat Biotechnol 38, 276-278, doi:10.1038/s41587-020-0439-x (2020).

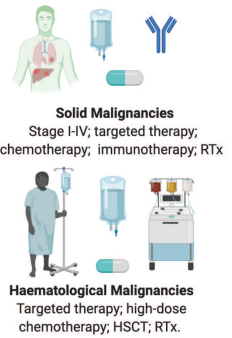
1078 51. Faulkner, N., et al., Reduced antibody cross-reactivity following infection with B.1.1.7 than  
1079 with parental SARS-CoV-2 strains. bioRxiv, 2021: p. 2021.03.01.433314.

1080 52. Rihn, S.J., et al., A plasmid DNA-launched SARS-CoV-2 reverse genetics system and  
1081 coronavirus toolkit for COVID-19 research. PLoS Biol, 2021. 19(2): p. e3001091.

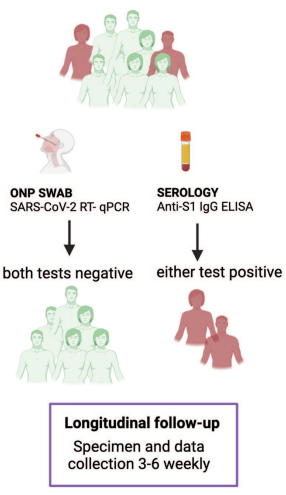
# a The CAPTURE Study

## PROSPECTIVE RECRUITMENT

- INCLUSION CRITERIA**
- >18 years in age
  - Any confirmed cancer diagnosis
- EXCLUSION CRITERIA**
- Condition that precludes informed consent

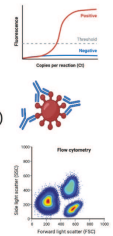


## SARS-CoV-2 CASE DEFINITION



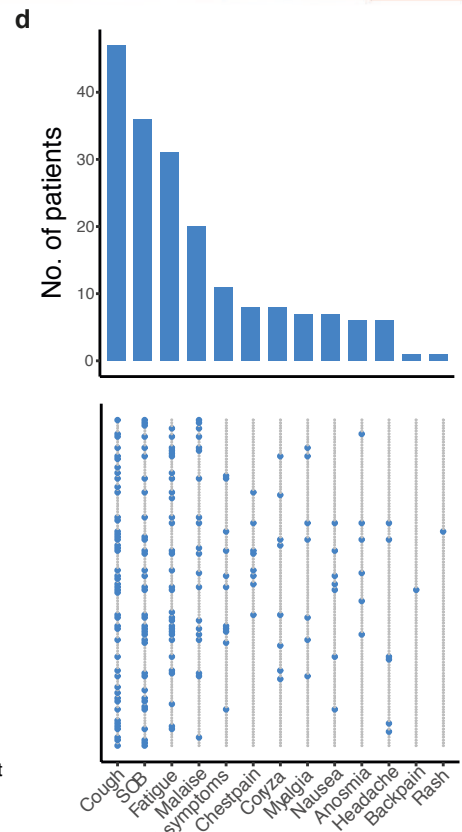
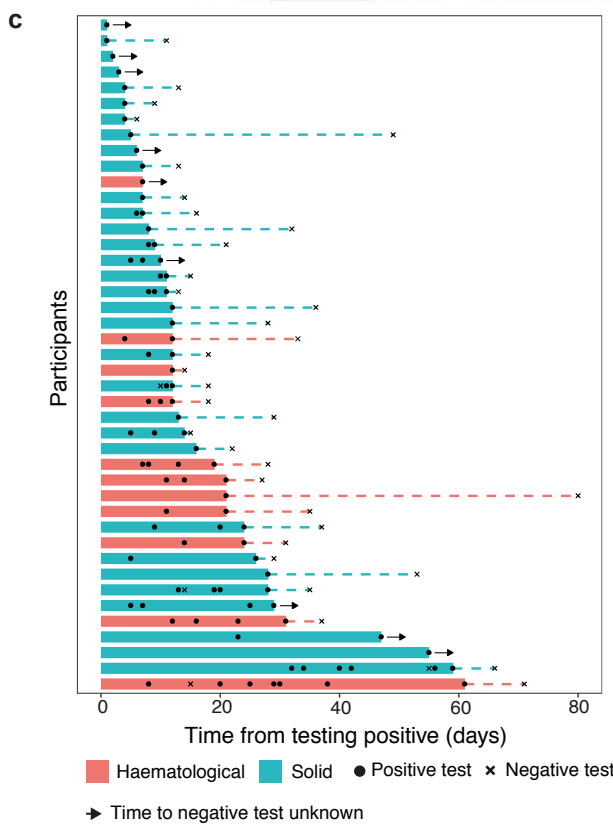
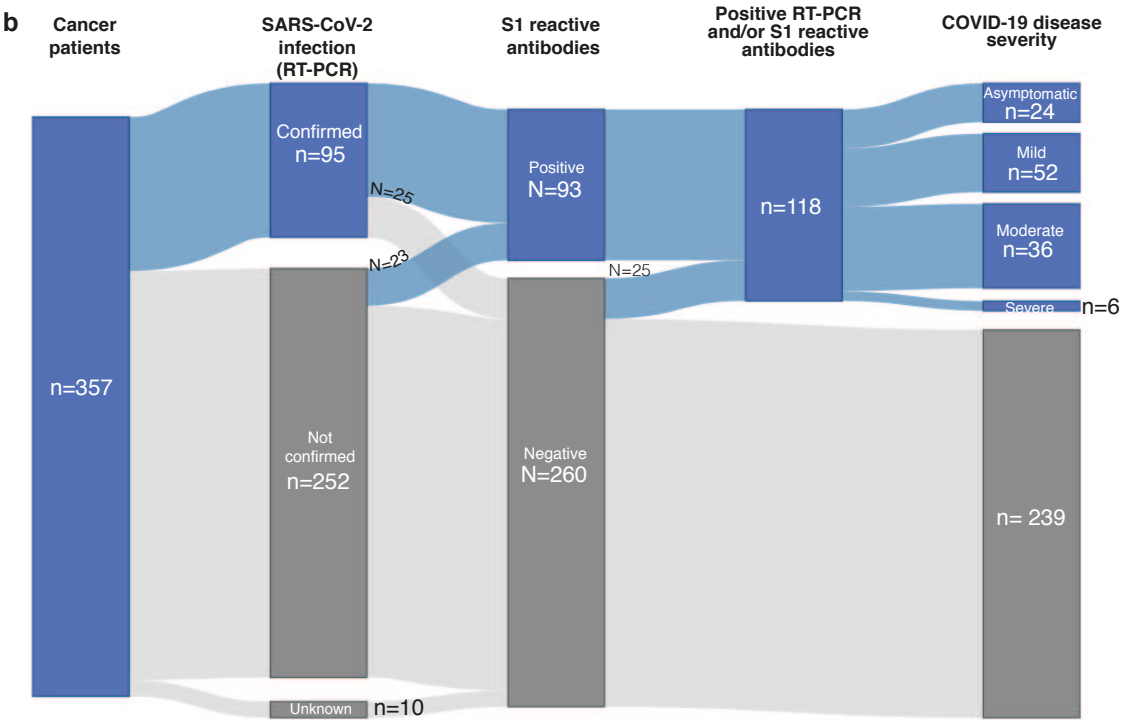
## BIOSPECIMENS & LABORATORY ASSAYS

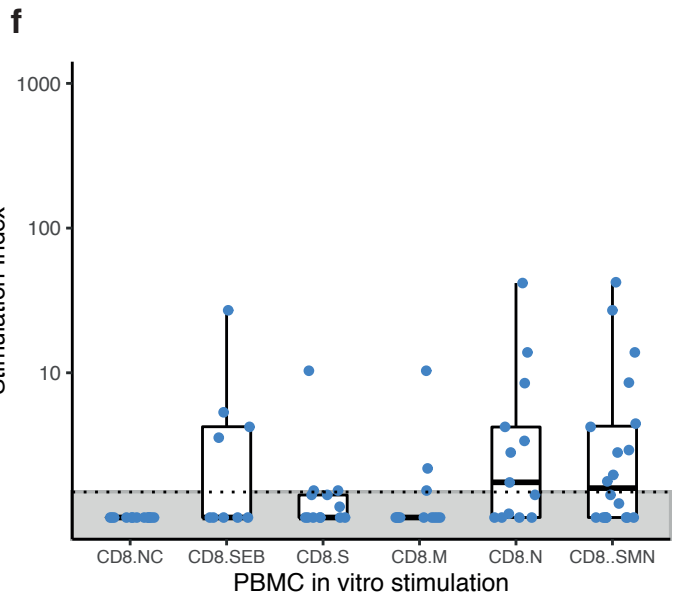
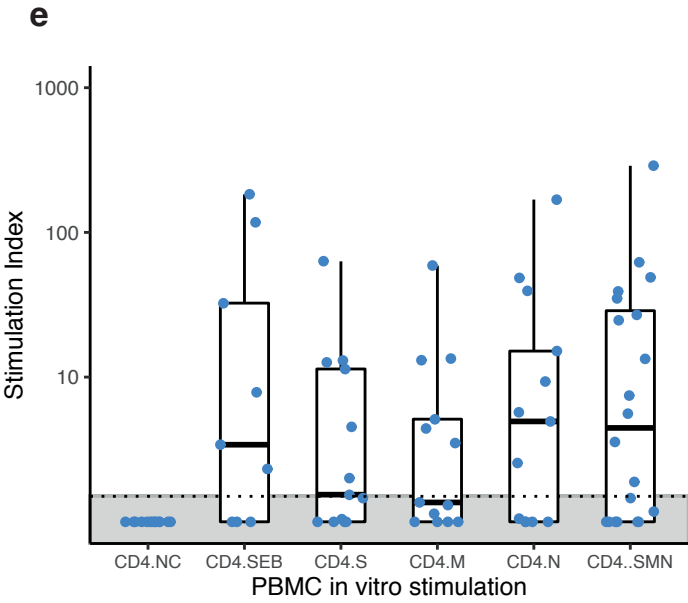
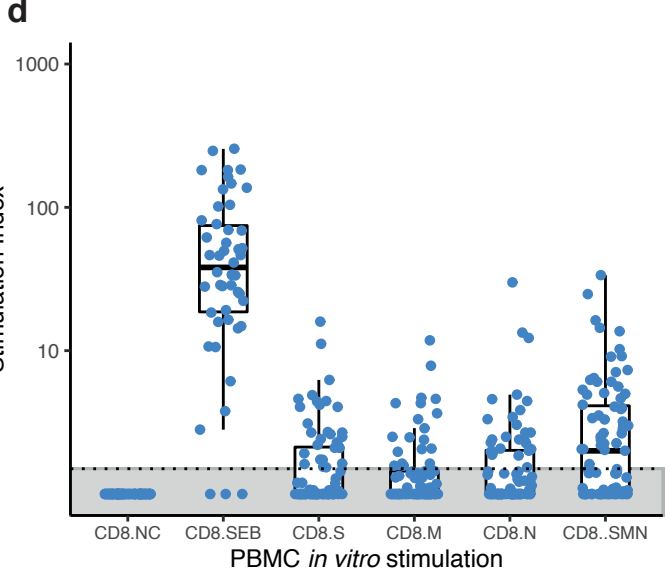
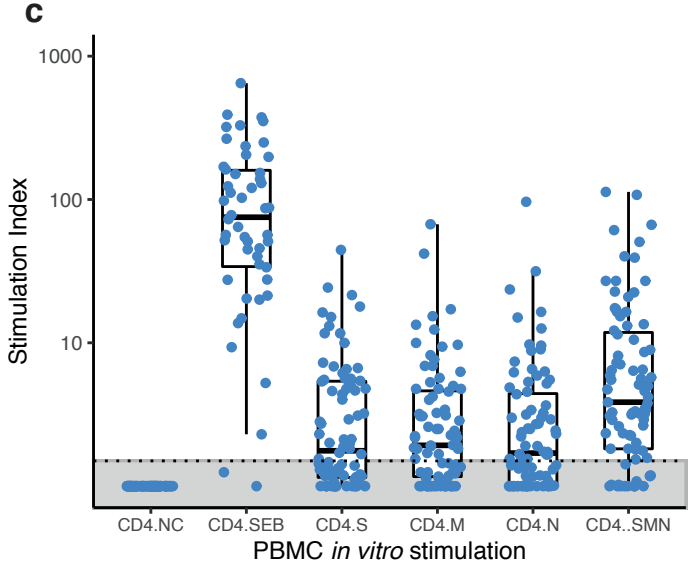
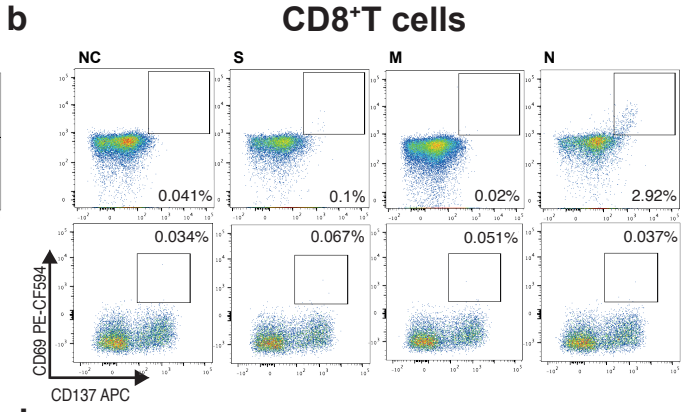
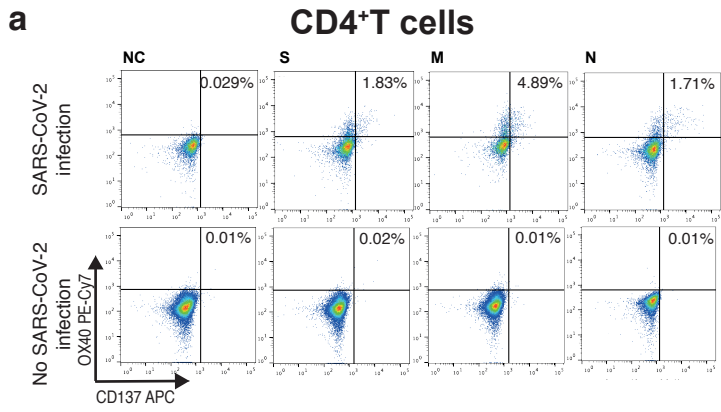
- ONP SWAB**
- SARS-CoV-2 RT- qPCR
  - SARS-CoV-2 WGS\*
- SERUM/PLASMA**
- Antibody response (ELISA & Flow)
  - Neutralising Ab response
  - Cytokine and chemokine profiling
- PBMCs**
- T-cell response & IFN-γ activation

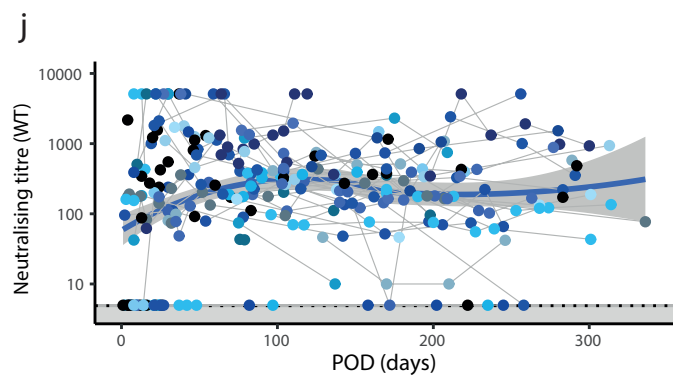
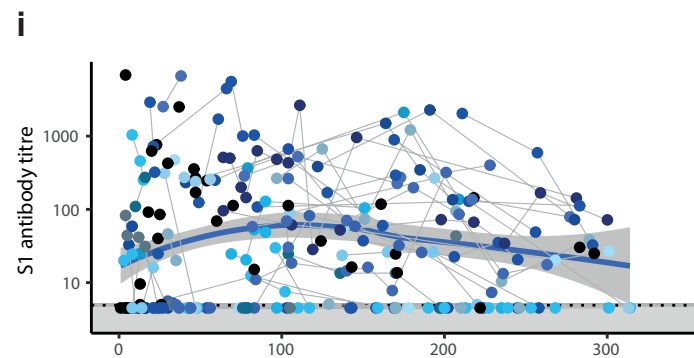
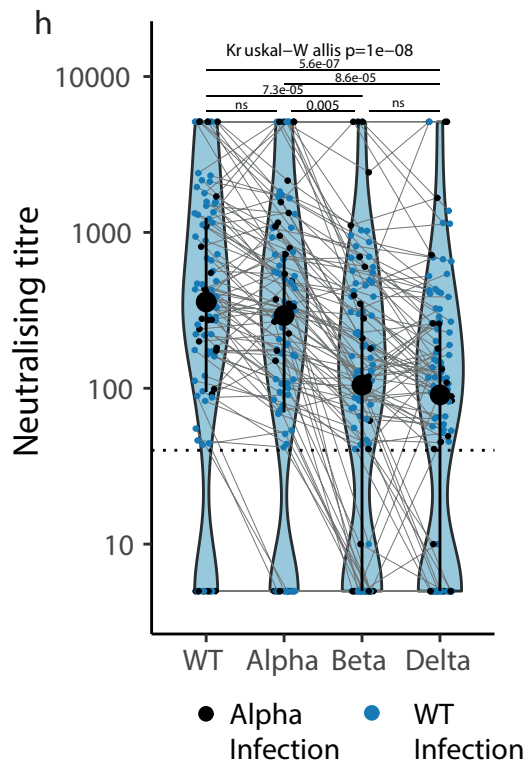
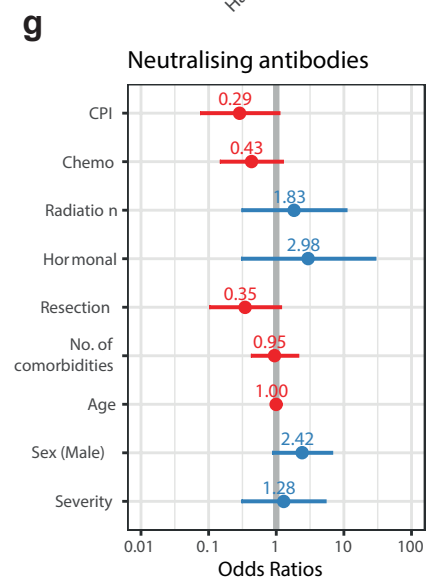
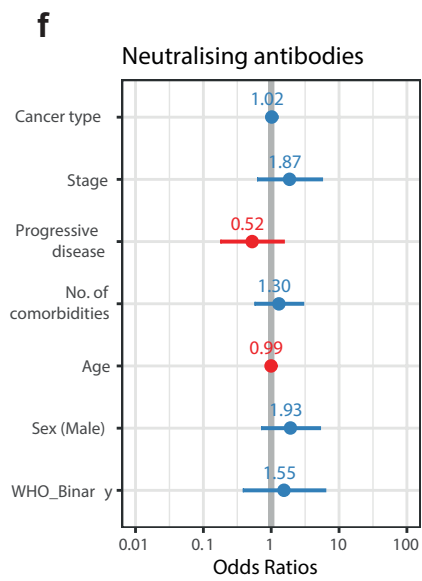
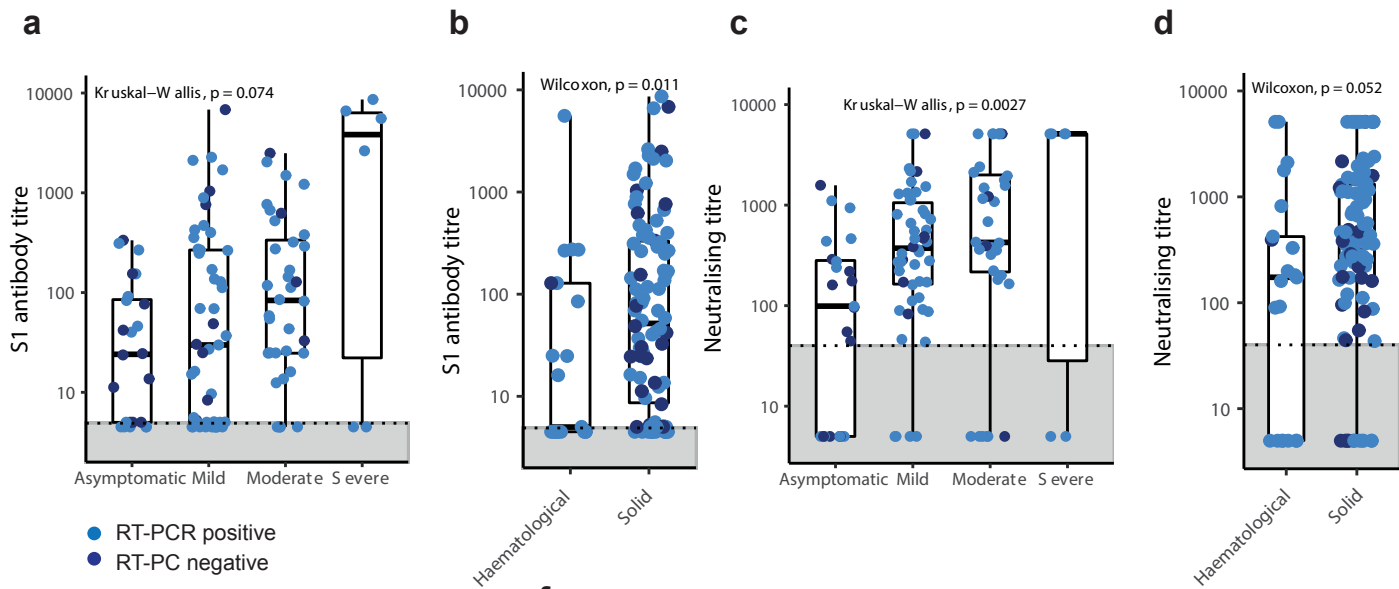


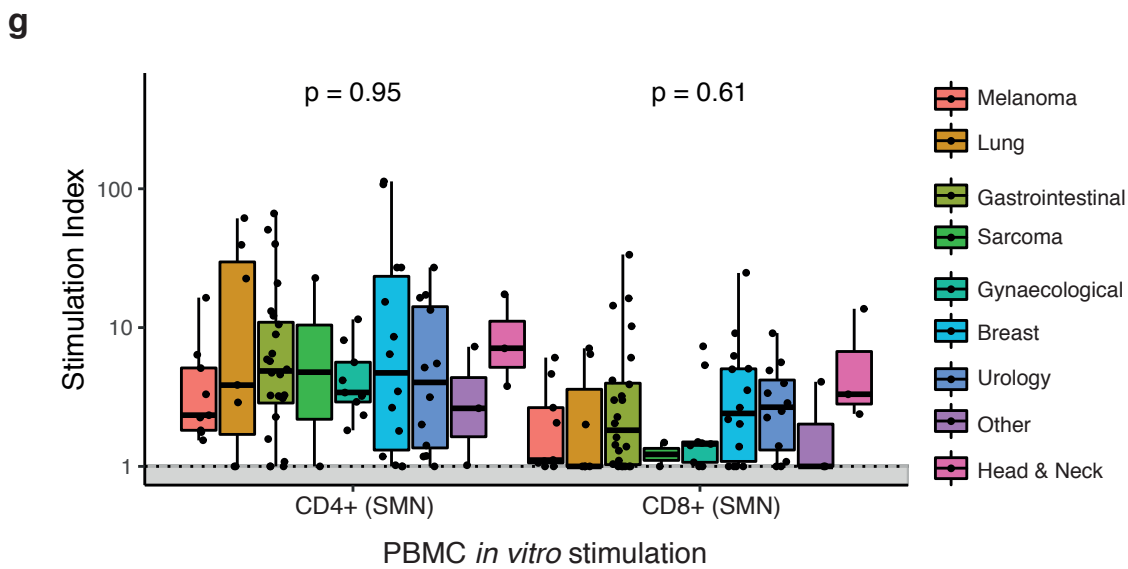
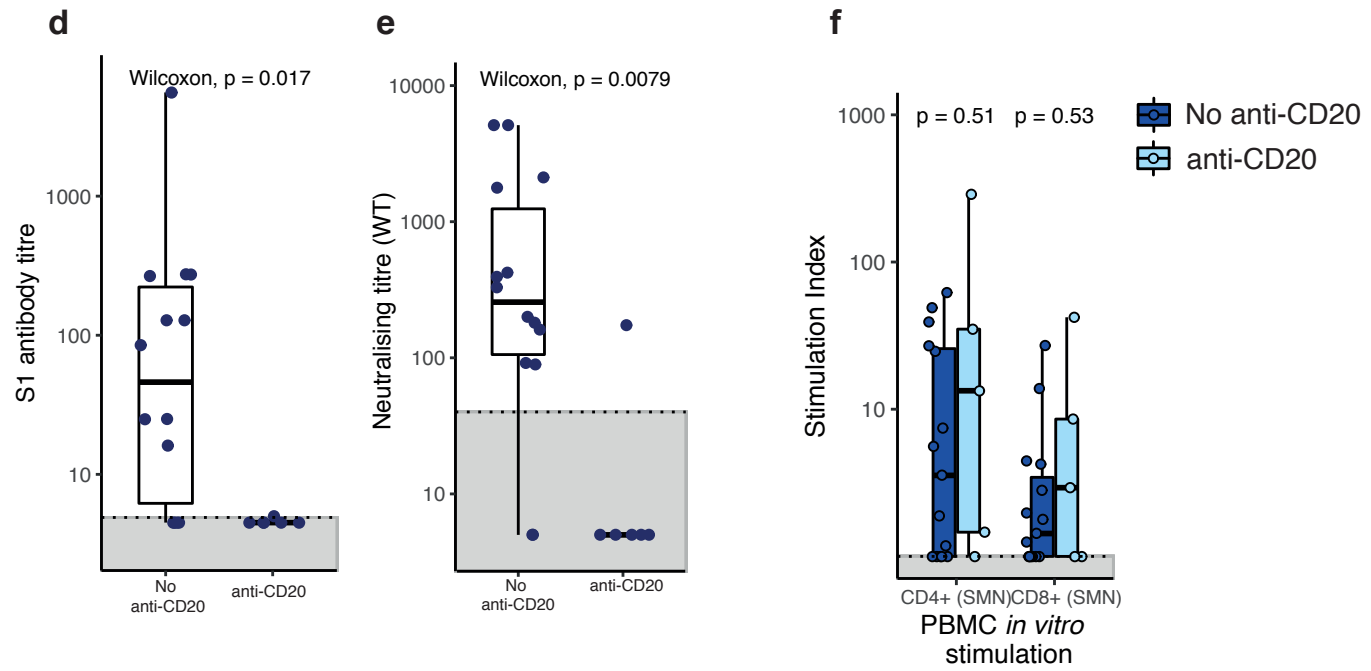
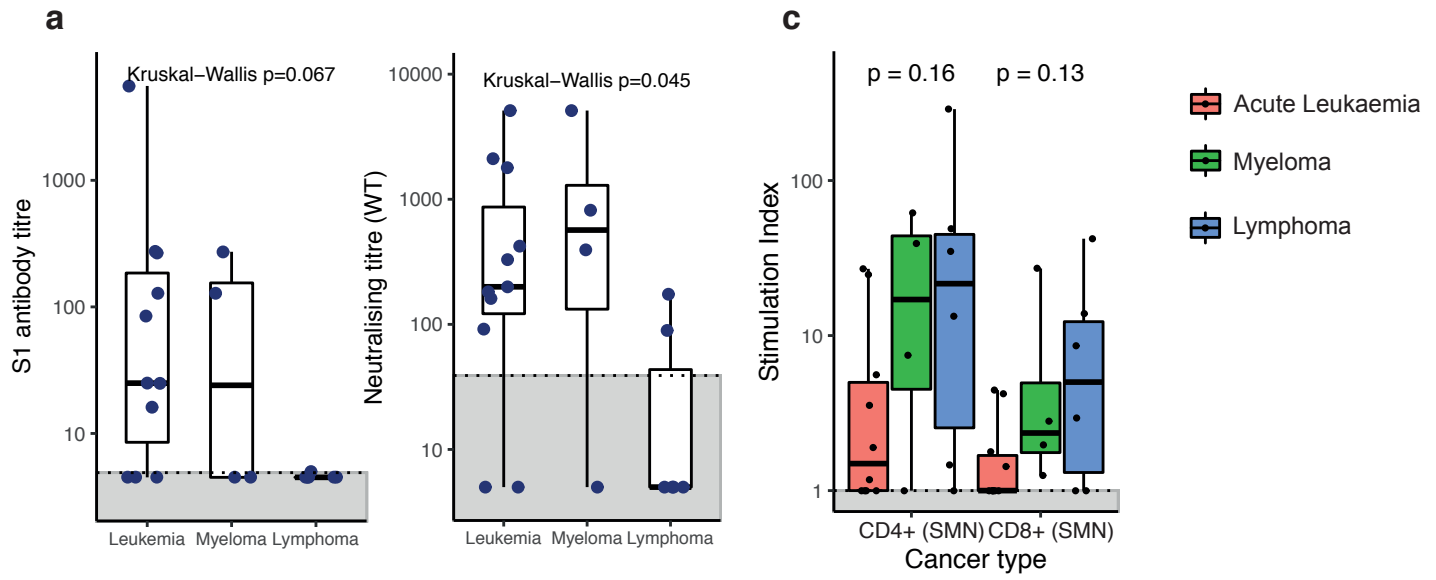
## COMPREHENSIVE DATA COLLECTION

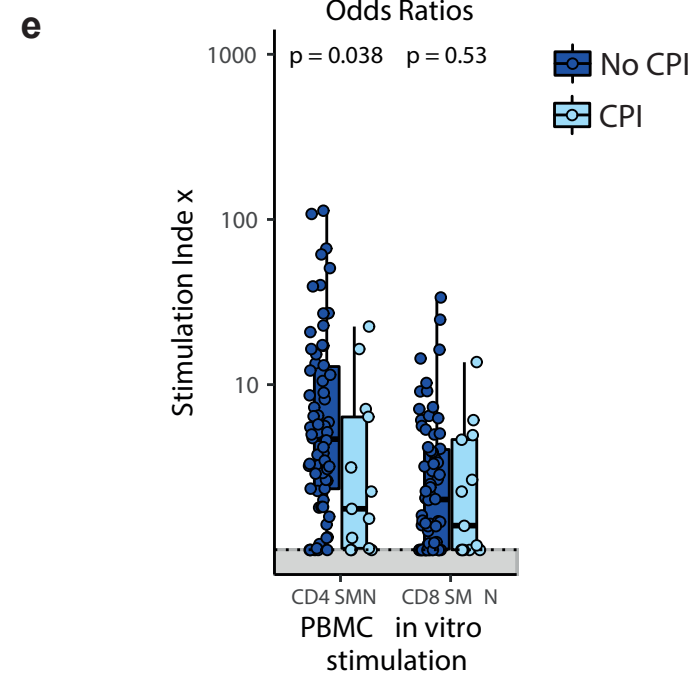
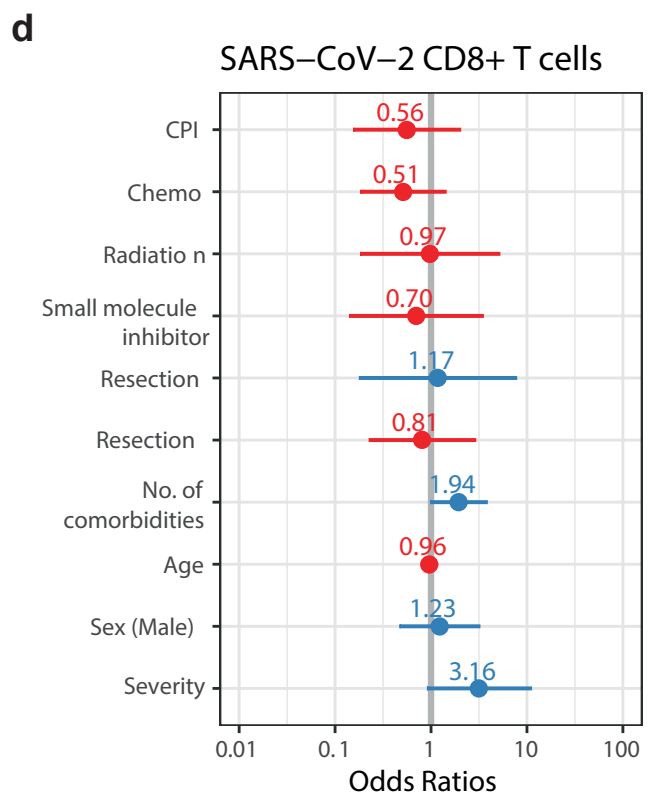
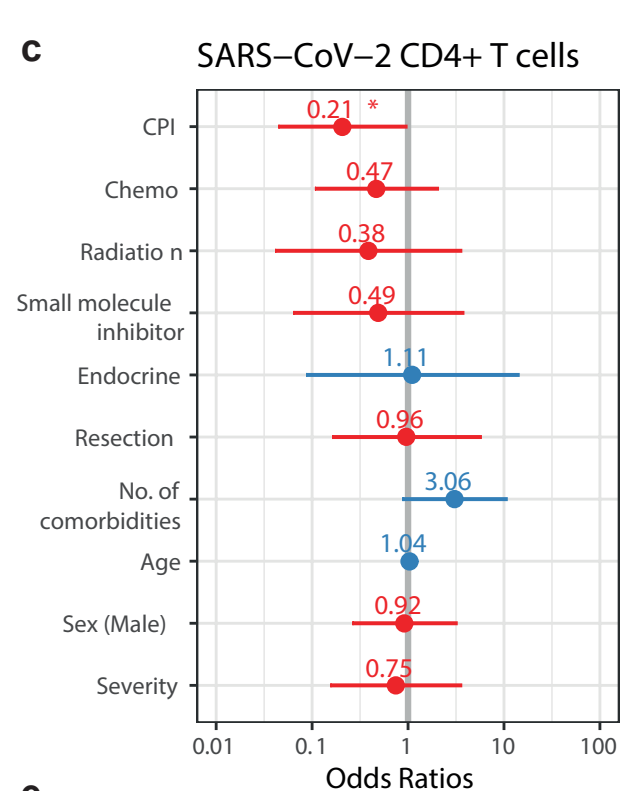
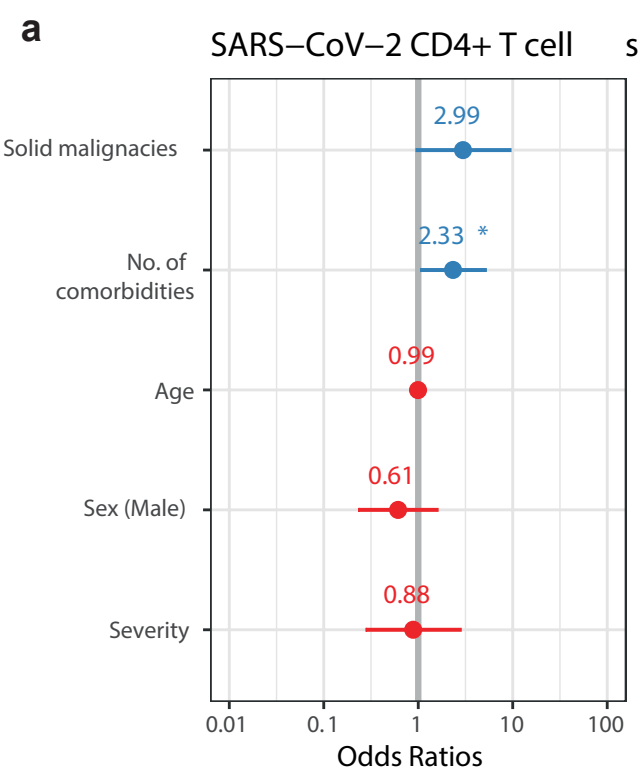
- Electronic Case Report Form (eCRF)**
- Containing 135 data points
  - Demographic and past medical history
  - Oncological treatment history
  - Standard of care diagnostic laboratory and radiology results













# Figures

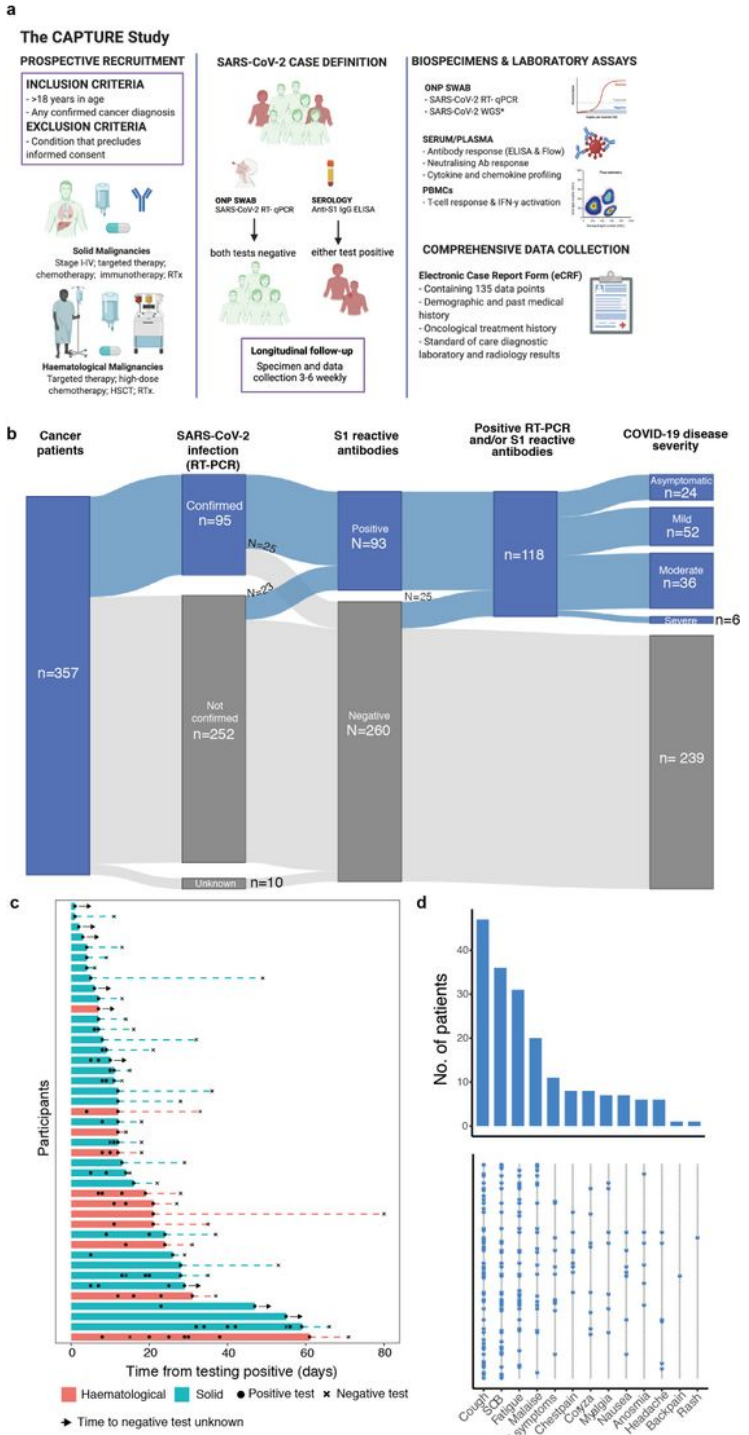


**Figure 1**

SARS-CoV-2 infection status, viral shedding, and COVID-19 symptoms of recruited patients. a) Patients with cancer irrespective of cancer type, stage, or treatment were recruited. Follow-up schedules for patients with cancer were bespoke to their COVID-19 status and account for their clinical schedules

(inpatients: every 2 – 14 days; outpatients: every clinical visit maximum every 3-6 weeks in year one and every six months in year two, and at the start of every or every-second cycle of treatment). Clinical data, oronasopharyngeal swabs and blood were collected at each study visit. Viral antigen testing (RT-PCR on swabs), antibody (ELISA, flow cytometric assay), T cell response and IFN- $\gamma$  activation assays were performed. b) Distribution of SARS-CoV-2 infection, and S1-reactive Ab status and COVID-19 severity in patients with cancer. 357 patients with cancer were recruited between May 4, 2020 and March 31st 2021. SARS-CoV-2 infection status by RT-PCR and S1-reactive Ab were analysed at recruitment and in serial samples. RT-PCR results prior to recruitment were extracted from electronic patient records. COVID-19 case definition includes all patients with either RT-PCR confirmed SARS-CoV-2 infection or S1-reactive Ab. c) Viral shedding in 43 patients with serial positive swabs. Solid bars indicate time to the last positive test, dotted lines denote the time from the last positive test to the first negative test. d) Distribution of symptoms in 118 COVID-19 patients. Bar graph denotes the number of patients. Each row in the lower graph denotes one patient. ONP, Oronasopharyngeal; ELISA, enzyme-linked immunoassay; PBMCs, peripheral blood mononuclear cells; WGS - whole genome sequencing, RTx, radiotherapy, HSCT, human stem cell transplant.

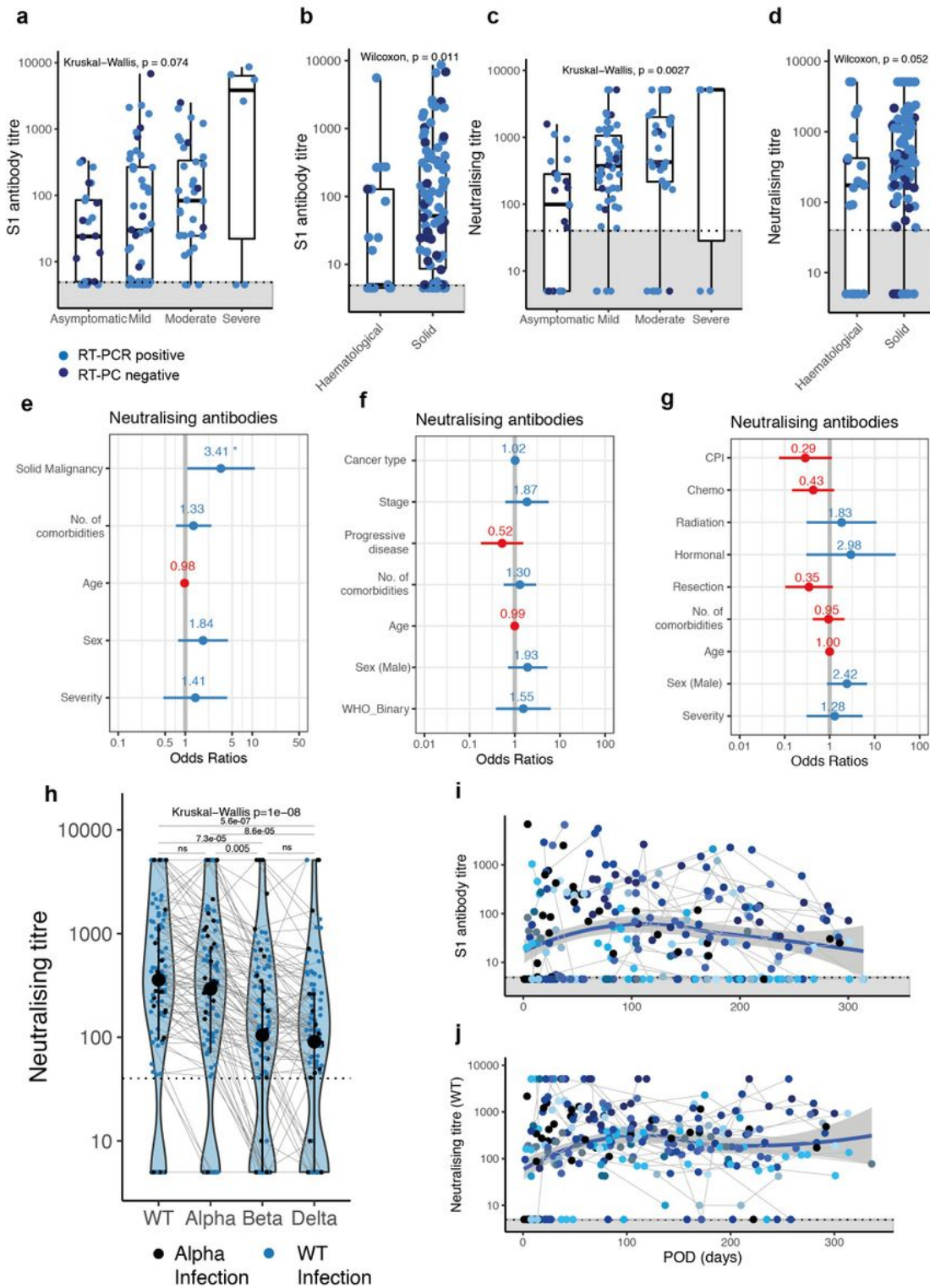


**Figure 2**

S1-reactive and antibody response in patients with cancer a) S1-reactive AbT by COVID-19 severity (n=112 patients). Significance was tested by Kruskal-Wallis test,  $p = 0.074$ . b) S1-reactive AbT by cancer type (Solid patients: n= 92, Haematological patients: n=20). Significance was tested by two-sided Wilcoxon Wilcoxon-Mann-Whitney U test,  $p = 0.011$ . c) NAbT by COVID-19 severity (n=112 patients). Significance was tested by Kruskal-Wallis test,  $p = 0.0027$ . d) NAbT by cancer type (Solid patient: n= 92,

Haematological patients: n=20). Significance was tested by two-sided Wilcoxon-Mann-Whitney U test,  $p = 0.052$ . Boxes indicate 25 and 75 percentiles, line indicates median, and whiskers indicate 1.5 times the IQR. Dots represent individual samples. Dotted lines and grey boxes denote the limit of detection. e) Multivariate binary logistic regression evaluating association with lack of NAb in patients with cancer (n=112). Wald z-statistic was used to calculate two-sided p-values. \*,  $p = 0.038$ . f) Multivariate binary logistic regression evaluating the association of lack of NAb in patients with solid cancer (n = 92). g) Multivariate binary logistic regression evaluating the association of lack of NAb in patients with solid cancer (n = 92). Dot denotes odds ratio (blue, positive odds ratio; red, negative odds ratio); whiskers indicate 1.5 times the IQR. h) NAbT against WT, Alpha, Beta, and Delta VOCs in patients (n=112) infected with WT SARS-CoV-2 or Alpha VOC. Violin plots denote density of data points. PointRange denotes median and 25 and 75 percentiles. Dots represent individual samples. Significance was tested by Kruskal Wallis test,  $p = 3.5e-07$ , two-sided Wilcoxon Mann Whitney U-test with Bonferroni correction (post-hoc test) was used for pairwise comparisons. p-values are denoted in the graph. i) S1-reactive AbT and j) NAbT post onset of disease (n=97 patients). Blue line denotes loess regression line with 95% confidence bands in grey. Black dots denote patients with one sample, coloured dots denote patients with serial samples (n=51 patients). Samples from individual patients are connected. Dotted lines and grey areas at bottom indicate limit of detection. NAb, neutralising antibody, NAbT, neutralising antibody titres, AbT, Antibody titres.

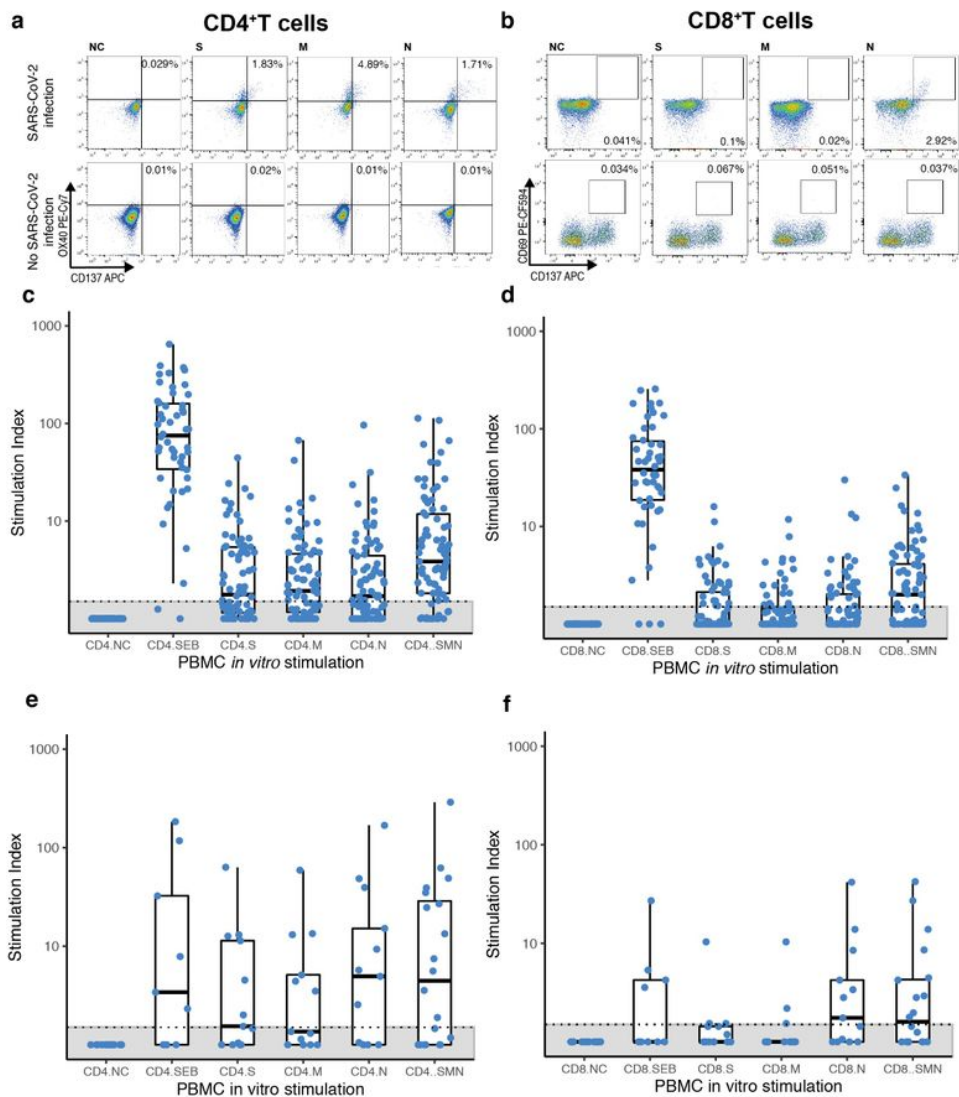


**Figure 3**

T cell response in patients with cancer a,b) Representative plots of CD4<sup>+</sup>CD137<sup>+</sup>OX40<sup>+</sup> (CD4<sup>+</sup>) and CD8<sup>+</sup>CD137<sup>+</sup>CD69<sup>+</sup> (CD8<sup>+</sup>) T cells in a patient with confirmed COVID-19 and a cancer patient without COVID-19 after *in vitro* stimulation with S, M, and N peptide pools, positive control (Staphylococcal enterotoxin B, SEB) or negative control (NC). Frequency of Sars-CoV-2-specific c) CD4<sup>+</sup> and d) CD8<sup>+</sup> T cells in solid patients with cancer (n= 83). Frequency of Sars-CoV-2-specific e) CD4<sup>+</sup> and f) CD8<sup>+</sup> T cells in haematological patients with cancer (n= 21). Stimulation index was calculated by dividing the

percentage of positive cells in the stimulated sample by the percentage of positive cells in the negative control (NC). To obtain the total number of SsT cells the sum of cells activated by S, M, and N was calculated (SMN). Boxes indicate the 25 and 75 percentiles, line indicates the median, and whiskers indicate 1.5 times the IQR. Individual patients are represented as dots. Dots represent individual samples. Dotted lines and grey boxes denote the limit of detection. SsT cells, Sars-CoV-2-specific T cells.

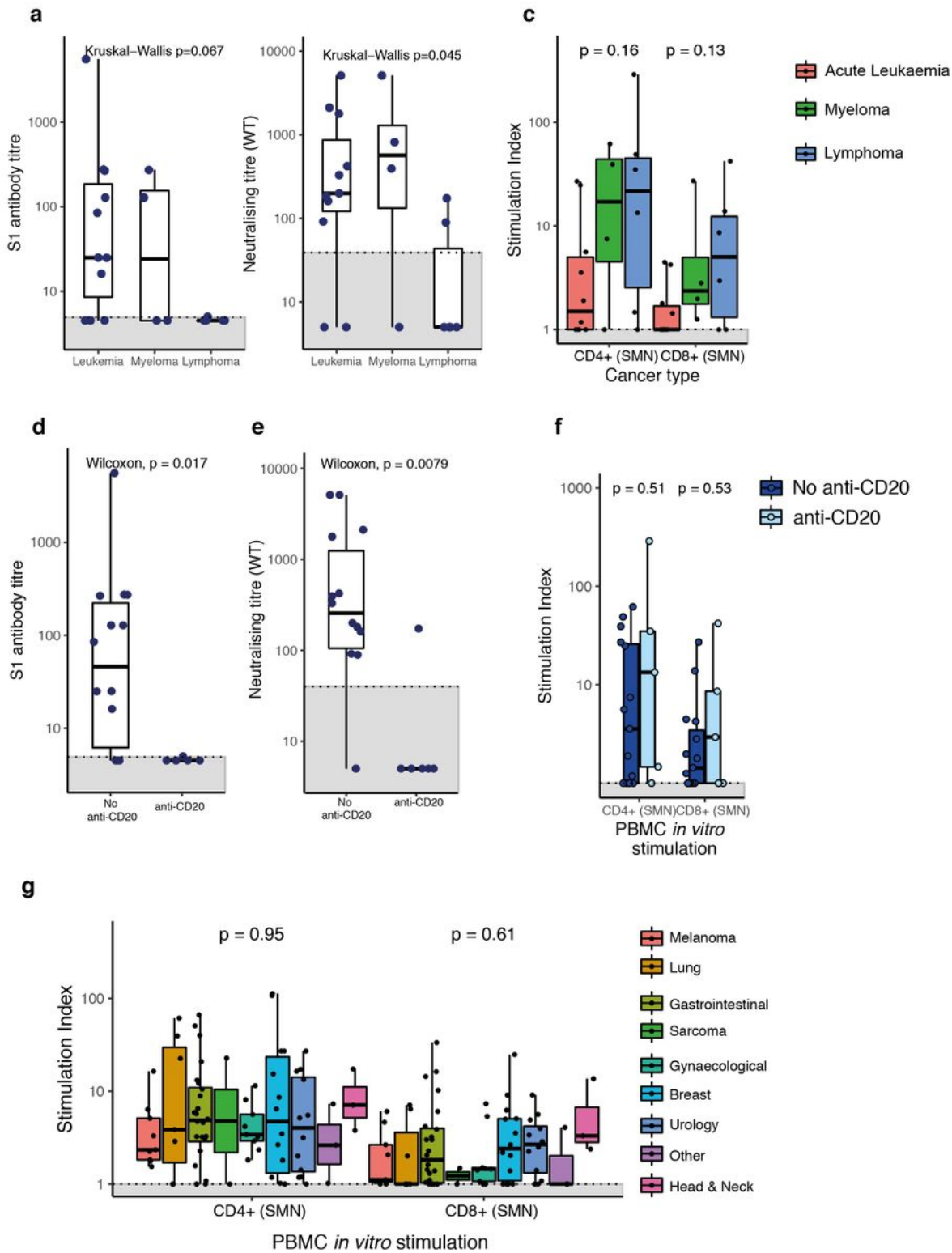
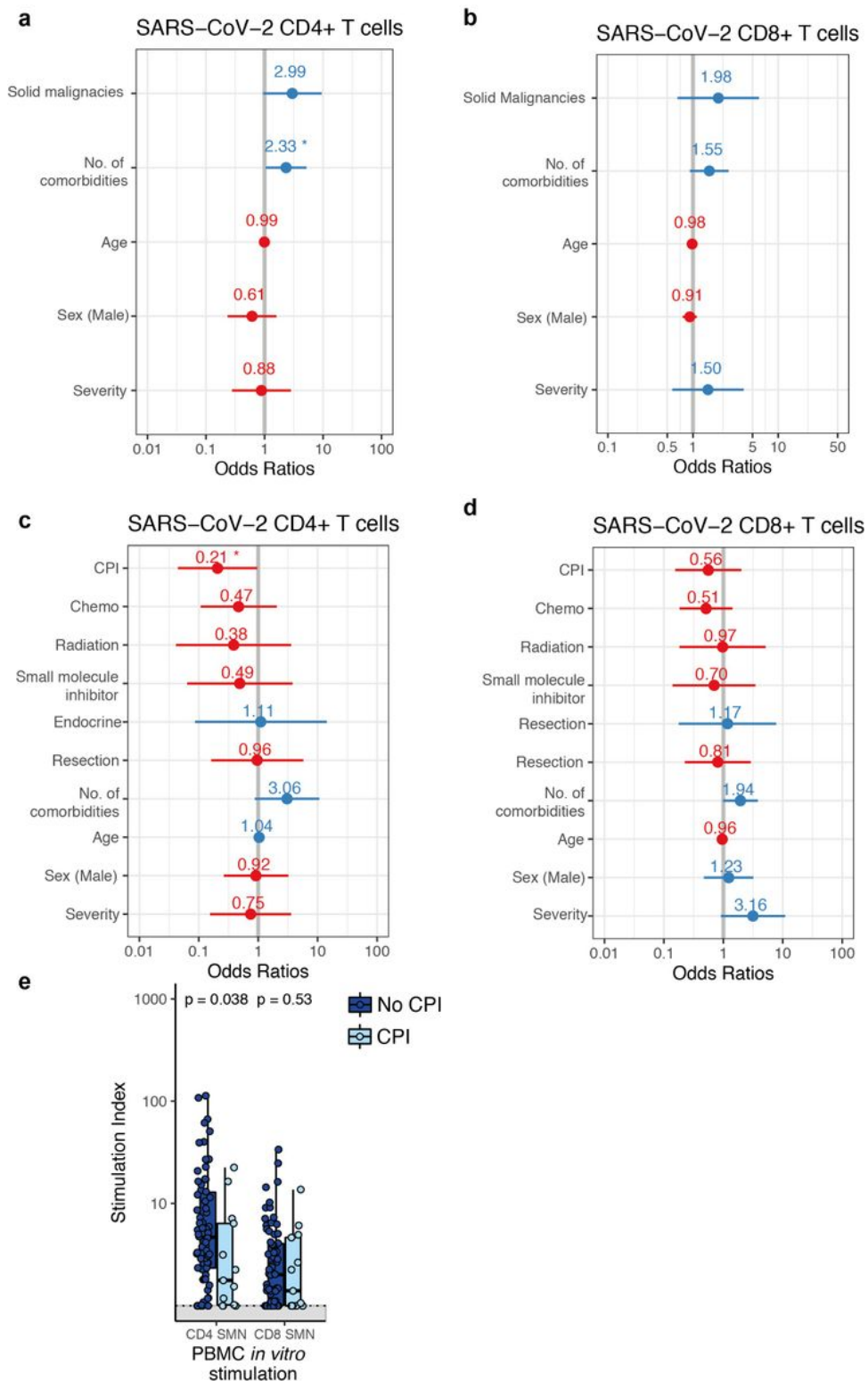


Figure 4

Comparison of antibody and T cell responses in patients with cancer a) S1-reactive AbT in patients with leukaemia (n=11), myeloma (n=4), and lymphoma (n=6). b) Neutralising antibody titres in patients with leukaemia (n=10), myeloma (n=4), and lymphoma (n=6). c) CD4+ and CD8+ cells T cells across patients with leukemia (n=10), myeloma (n=4), or lymphoma (n=6). Stimulation index was calculated by dividing the percentage of CD4+CD137+OX40+ (CD4+) and CD8+CD137+CD69+ (CD8+) T cells in the stimulated sample by the percentage of positive cells in the negative control (NC). Significance was tested by Kruskal-Wallis test,  $p < 0.05$  was considered significant. d) S1-reactive AbT in patients with haematological malignancy receiving anti-CD20 treatment (n=6) vs other SACT (n=15). e) NAbT in patients with haematological malignancy receiving anti-CD20 treatment (n=6) vs other SACT (n=15). Significance was tested by two-sided Wilcoxon-Mann-Whitney U test,  $p < 0.05$  was considered significant. f) Comparison of CD4+/CD8+ T cells between patients with haematological malignancies on anti-CD20 therapy (n=5, administered within six months) and not on anti-CD20 therapy (n=15). Significance was tested by two-sided Wilcoxon-Mann-Whitney U test,  $p < 0.05$  was considered significant. g) CD4+ and CD8+ cells T cells across patients with solid cancer (n=81) by cancer subtype. Boxes indicate the 25 and 75 percentiles, line indicates the median, and whiskers indicate 1.5 times the IQR. Dots represent individual patient samples. Dotted lines and grey boxes denote the limit of detection. Significance was tested by Kruskal-Wallis test,  $p < 0.05$  was considered significant. SACT, systemic anti-cancer therapy.



**Figure 5**

Associations between SARS-CoV-2-specific T cells with patient or cancer-specific features Multivariate binary logistic regression analysis evaluating associations between SARS-CoV-2-specific a) CD4+ and b) CD8+ T cells with cancer diagnosis (solid vs haematological malignancies), comorbidities, age, sex, and COVID-19 disease severity in 100 patients. Wald z-statistic was used to calculate two-sided p-values. \*,  $p = 0.038$ . Multivariate binary logistic regression analysis evaluating associations between SARS-CoV-2-



specific c) CD4+ and d) CD8+ T cells with anti-cancer intervention, age, sex, and COVID-19 disease severity in patients with solid cancer (n=81). Wald z-statistic was used to calculate two-sided p-values. \*,  $p = 0.045$ . Dot denotes odds ratio (blue and red dots indicate positive or negative odds ratio, respectively) ; whiskers indicate 1.5 times the IQR. e) Comparison of SARS-CoV-2-specific CD4+/CD8+ T cells between patients with solid malignancies on CPI (n=13, administered within three months) and not on CPI (n=68). Boxes indicate the 25th and 75th percentiles, line indicates the median, and whiskers indicate 1.5 times the IQR. Dots represent individual samples. Significance was tested by two-sided Wilcoxon-Mann-Whitney U test ( $p = 0.038$  and  $0.53$ ).

## Supplementary Files

This is a list of supplementary files associated with this preprint. Click to download.

- [ExtendedFigure1infection.png](#)
- [ExtendedFigure2infection.png](#)
- [ExtendedFigure3Infection.png](#)
- [ExtendedFigure4Infection.png](#)
- [ExtendedFigure5Infection.png](#)
- [ExtendedFigure6infection.png](#)
- [SupplementaryTable1infection.pdf](#)
- [SupplementaryTable2infection.pdf](#)
- [SupplementaryTable3Infection.pdf](#)